Estimating the Abundance of Outmigrant Juvenile Chinook Salmon from Rotary Screw Traps on Tributaries of the Sacramento River, California

Authors

Josh Korman, Ecometric Research; Liz Stebbings, FlowWest; Ashley Vizek, FlowWest; Brett Harvey, California Department of Water Resources; Erin Cain, FlowWest

Acknowledgments

The data used in this modeling effort are rich and extensive; in some cases, data collection has been ongoing since the late 1990s. This work would not be possible without field staff collecting daily rotary screw trap data and the data stewards that have managed these data over time. We gratefully recognize: Jason Kindopp, Feather River; Kassie Hickey, Feather River; Ryan Revnak, Mill and Deer Creek; Casey Campos, Yuba River; Mike Shraml, Battle and Clear Creek; Natasha Wingerter, Battle and Clear Creek; and Grant Henley, Butte Creek.

We also thank the Spring-run Juvenile Production Estimate Core Team, Modeling Advisory Team, and Interagency Review Team for their useful comments and advice.

Work by Ecometric Research and FlowWest on this project was supported by California Department of Water Resources.

Executive Summary

In 2020, an Incidental Take Permit (ITP) was issued to the California Department of Water Resources (DWR) by the California Department of Fish and Wildlife for operation of the State Water Project. Condition of Approval (COA) 7.5.2 of this permit requires DWR to lead an interagency Core Team, develop a modeling approach for calculating annual juvenile production estimates (JPE) for spring-run Chinook salmon (*Oncorhynchus tshawytscha*) (spring-run) produced in the Sacramento River watershed. This chapter describes an important step toward this objective: the estimation, for all years having adequate historical data, of spring-run outmigrant abundance at all rotary screw trap (RSTs) sites in Sacramento River tributaries where spring-run are present. These outmigrant abundance estimates will be used to fit (i.e., calibrate parameters of) multiple candidate JPE models. The abundance estimates and the dataset assembled to produce them will also be used to improve the structure and accuracy of other existing and future models guiding resource management in California's Central Valley, including the suite of salmon life cycle models produced by the interagency Science Integration Team, a technical group tasked with guiding restoration funding of the Central Valley Project Improvement Act. In addition, this chapter will aid the Core Team with an additional required task: reviewing data produced by spring-run monitoring programs in the Sacramento River watershed, and recommending adjustments and augmentations to that monitoring to improve the ability of monitoring data to support calculation of an annual JPE.

An extensive network of RSTs is used to monitor the abundance of outmigrant juvenile Chinook salmon from streams and rivers in the Central Valley of California. To estimate the abundance of outmigrants over a trapping period each year (i.e., a run year), catches are expanded (i.e., divided) by the estimated proportion of fish that are captured when passing the trap. This proportion, commonly referred to as trap efficiency or capture probability, can be estimated from efficiency trials based on mark-recapture. A variety of statistical modeling approaches can be used to convert catch and efficiency trial data into estimates of capture probability and abundance. However, there is no agreed-upon method for Central Valley RST data. This limits the utility of RST information for many important goals, including development of a JPE for spring-run from the Sacramento River and its tributaries.

This chapter describes a new model that estimates abundance of juvenile Chinook salmon outmigrant abundance to support development of the spring-run JPE model.

Most RST programs use a two-sample mark-recapture approach to estimate abundance of outmigrant juvenile salmon and steelhead (*Oncorhynchus mykiss*). Fish are initially captured, marked and released upstream of the RST during the first sampling period. A second sample is then taken from the population, which consists now of both marked and unmarked fish. The ratio of marked fish

recaptured on the second sample to the number of marked fish released on the first sample is used to calculate capture probability during the second sampling period. The number of unmarked fish on the second sample can then be expanded (i.e., divided) by the capture probability to estimate the total number of unmarked fish passing the trap. The Peterson estimate is the simplest approach for analyzing such data; it calculates abundance by dividing the total number of unmarked fish caught over the trapping season by the average capture probability of the trap as determined by all efficiency trials over the trapping season. However, this unstratified Peterson estimate inherently assumes capture probability does not vary over the trapping season, as we might expect would occur due to changes in flow, water temperature, turbidity, or other factors. The stratified Peterson estimator calculates abundance over shorter time intervals such as a week, and then sums the weekly estimates to generate an annual value for the run year. This approach avoids the assumption that capture probability is constant over time. However, it is a data-intensive approach because it requires efficiency trial data (release of marked fish) for all weeks in a trapping season. There are typically only a limited number of trap efficiency trials within a run year for the majority of RST sites in Central Valley streams, so applying a stratified Peterson estimator to the data to estimate abundance for the entire run year is not possible.

To address challenges with data limitations in RST programs, Bonner and Schwarz (2011) developed the Bayesian Temporally Stratified Population Analysis System (BT-SPAS). This hierarchical Bayesian model (HBM) estimates capture probability for each stratum (e.g., week) in a trapping season based on the available efficiency trial data for that season. The approach provides a way to estimate capture probability when there are missing efficiency trial data for some weekly strata. BT-SPAS uses a spline method to estimate abundances, which improves precision of abundance estimates when there is missing efficiency trial data or where existing efficiency trial data is uninformative. The BT-SPAS spline approach does not assume weekly abundance estimates are completely independent over time (i.e., over strata) like the stratified Peterson estimator does, so it can also estimate abundance in strata that are not sampled. BT-SPAS was originally developed for analyzing juvenile Chinook salmon RST data from the Trinity River in California (Schwarz et al. 2009, Som and Pinnix 2014), and has since been applied to other rivers in the Central Valley (e.g., Pilger et al. 2019) and elsewhere.

Data from Central Valley RST programs have some unique limitations that preclude the use of BT-SPAS for the majority of RST site-run year cases. Thus, we developed a modified version of BT-SPAS, called BT-SPAS-X, using “X” for extension) to address these limitations in the Central Valley RST data. The main advancement with the BT-SPAS-X model is that, when estimating abundance for a particular run year and RST site, it uses efficiency trial data from all years for that site. Owing to this approach, BT-SPAS-X provides more reliable estimates of capture probability and abundance in the majority of years when no or a limited number of efficiency trials are available. By considering efficiency trial data from all sites in the same

model, BT-SPAS-X estimates the across-site variation in capture probability, which allows prediction of capture probability and abundance at sites with no efficiency trial data.

We applied BT-SPAS-X to 15 RST sites from seven Sacramento River tributaries (Battle, Clear, Mill, Deer and Butte creeks, and Feather and Yuba rivers) where spring-run are present. The model estimated outmigrant juvenile Chinook salmon abundance based on the combined catch of fry and smolts for all run types. The capture probability component of the model was fit to data from 1,056 efficiency trials across 14 RST sites. The capture probability model included effects of site location and flow. The estimated grand mean of capture probability across sites was approximately 0.025 (i.e., 2.5%). There was a negative effect of increasing flow on capture probability. Capture probability of hatchery-origin marked releases was approximately 50% lower than capture probability for natural-origin releases. However, origin of release was only recorded for 91 of 1,056 release trials (9%), so this effect could not be included in the model. Surprisingly, there was no relationship between average fork length of marked releases and capture probability based on 467 trials where fork length was recorded, so fish size was not included as a covariate in the model.

While the hierarchical model accounted for 99% of the variation in capture probabilities observed across 1,056 efficiency trials, much of this variation was explained by random effects. These effects do not contribute to the predictive ability of the model when it is applied to the majority of weekly strata that do not have trap efficiency data. Random effects are simulated for weeks without efficiency data, leading to considerably greater uncertainty in capture probability compared to weeks with efficiency data. For example, in Battle Creek, the predicted capture probability in weeks with efficiency trial data at average flow was approximately 0.05 with 95% credible intervals spanning approximately 0.04–0.06. In contrast, in weeks with average flow but no efficiency trial data, the 95% credible intervals ranged from approximately 0.02–0.15.

We estimated weekly capture probability, and weekly and annual outmigrant abundance (all Chinook run types combined) for 170 different RST site-run year cases. We modeled a 31-week run year from November 4 through May 27. We compared weekly predictions of capture probability and abundance from BT-SPAS-X with stratified Peterson estimates for weeks when they were available. Generally, the model matched the Peterson estimates very well, and it appears to make reasonable predictions for weeks that were not sampled or where efficiency trial data were not available. Relative precision (that is, the coefficient of variation, or CV) of annual abundance estimates averaged 26% across all RST sites and run years. Mean precision of annual abundance estimates across RST sites ranged from 21–41%. There was also considerable variation in precision across run years within RST sites. This variation was driven by the number of efficiency trials available, the overlap weeks with both efficiency trials and high catch, and the patchiness of

weekly abundance estimates within run years. In general, uncertainty in the annual abundance estimate was higher in years when the majority of the annual abundance was concentrated in a limited number of weeks.

Estimates of the combined abundance of all run types of Chinook salmon by RST site and week were converted to weekly estimates of spring-run abundance based on estimated proportions of spring-run. These latter estimates were derived from the probabilistic length-at-date (PLAD) model. There was strong seasonal variation in the proportion of spring-run across weeks, but relatively precise estimates of the proportion for any week. The uncertainty in the spring-run estimates was sometimes greater than the all run type estimate because the precision of the proportion predicted by PLAD could be relatively high. However, this effect varied by RST site and was minimal when spring-run proportions were high (e.g., in upper Clear Creek, or at Parrot-Phelan Dam).

Contents

Tables

Figures

Appendices

A. Predictions of Weekly Capture Probabilities, Chinook Salmon Abundances (All Runs)

B. Predictions of Weekly Probabilistic Length-at-Date Predictions and Spring-run Abundances

Acronyms and Abbreviations

Term	Definition
AIC	Aikake Information Criteria
BT-SPAS	Bayesian Temporally Stratified Population Analysis System
BUGS	Bayesian inference using Gibbs sampling
CAMP	Comprehensive Assessment and Monitoring Program
CAMPR	Comprehensive Assessment and Monitoring Program in R
CV	coefficient of variation
DAG	directed acyclic graph
DWR	California Department of Water Resources
HBM	hierarchical Bayesian model
ITP	Incidental Take Permit
JPE	juvenile production estimate
LCC	lower Clear Creek
PLAD	probabilistic length-at-date
RST	rotary screw trap
SPAS	Stratified Population Analysis System
spring-run	spring-run Chinook salmon
SWP	State Water Project
UBC	upper Battle Creek
UCC	upper Clear Creek

1 Introduction

Rotary screw traps (RSTs) are commonly used in streams and rivers to monitor the abundance of outmigrating juvenile Chinook salmon (*Oncorhynchus tshawytscha*) and steelhead (*Oncorhynchus mykiss*). An extensive network of RSTs is used to monitor the abundance of outmigrating juvenile Chinook salmon from streams in California's Central Valley. To estimate the abundance of outmigrants over a trapping period each year, catches are expanded (i.e., divided) by the estimated proportion of fish that are captured when passing the trap. This proportion, commonly referred to as trap efficiency or capture probability, can be estimated from efficiency trial data. Efficiency can be challenging to estimate, and data to estimate efficiency are frequently unavailable. A variety of statistical modeling approaches can be used to convert catch and efficiency estimates into abundance, but there is no agreed-upon method for estimating outmigrant abundance from Central Valley RST data, though efforts have been made (McDonald and Mitchell 2020). This limits the utility of the RST data to evaluate differences in outmigrant juvenile abundance across tributaries and changes over time. This in turn limits the utility of RST information for many important goals, including development of a juvenile production estimate (JPE) for spring-run Chinook salmon (spring-run) from the Sacramento River and its tributaries.

This chapter describes a model that was developed to estimate weekly and annual abundance of outmigrating Chinook salmon juveniles (for all run types combined and only spring-run) based on RST data from tributaries of the Sacramento River. We begin by providing background on how abundance estimates are typically estimated from RST data (Section 2). We then outline specific limitations of Central Valley RST data (Section 3), and describe a new model that can estimate outmigrant abundance given these limitations (Section 4). We present results that highlight key aspects of model behavior and show how well predictions of capture probability and abundance fit the data (Section 5). We end by identifying future work on the data and the model (Section 6). We also compare the model presented here with a previous effort (McDonald and Mitchell 2020), and discuss characteristics of a future model that could be applied to mainstem Sacramento River RST data. Annual and weekly outmigrant abundance estimates will be an important component of the spring-run JPE modeling effort. These abundance estimates would also be available to researchers with other objectives, such as life cycle modeling.

2 Background

This section briefly describes mark-recapture approaches and provides background and context needed to understand the model developed to analyze Central Valley RST data (Section 4).

Central Valley RST programs use a two-sample mark-recapture approach to estimate abundance of outmigrating juvenile Chinook salmon (Figure 1). Fish are initially captured, marked and released during a first sample. A second sample is then taken from the population that now consists of both marked and unmarked fish. The number of marked and unmarked fish in the second sample is then used to estimate the capture probability and abundance of fish that passed the trap location. A variety of methods can be applied to this temporally stratified mark-recapture data to estimate capture probability and abundance.

2.1 Unstratified Peterson Estimate

The simplest approach for estimating abundance from RST data is to divide the total number of unmarked fish caught over the trapping season by the trap efficiency:

Equation 1.

$$U = \frac{u}{p}, p = \frac{r}{R},$$

Where:

U is the estimated abundance of the unmarked population

u is the catch of unmarked fish, and

p is the trap efficiency, more commonly referred to in the mark-recapture literature as capture probability (the proportion of animals captured).

Capture probability is estimated as the ratio of the number of marked fish that are recaptured relative to the number of marked fish that are released, which we refer to here as efficiency trial data. This model is more generally referred to as a two-sample closed population model. The model is "closed" because it assumes that all fish that are marked and released above a trap migrate pass the trap. That is, there are no losses due to mortality prior to fish passing the trap, and that all fish resume their downstream migration after release.

2.2 Temporally Stratified Peterson Estimate

A critical assumption of the unstratified Peterson estimate is that capture probability does not vary over the entire period when the trap is operated (i.e., a trapping season from say November through May). In the case of the Central Valley tributaries, river conditions (e.g., flow and turbidity) can vary substantially over the trapping season, and these changes are expected to cause considerable variation in capture probability. In more general mark-recapture terms, the unstratified model does not account for heterogeneity (variability) in capture probability. As a result, the estimate of abundance has the potential to be substantively biased, and the uncertainty in the abundance estimate substantively underestimated. To address this very significant limitation, a stratified estimator is used:

Equation 2.

$$U_t = \frac{u_t}{p_t}, p_t = \frac{r_t}{R_t}, U = \sum_{t=1}^{t=T} U_t,$$

Where:

t is an index for each timestep (e.g., week).

Here the abundance for the entire trapping period (e.g., weeks 1 to the last week T) is simply the sum of estimates across timesteps. Note this model allows capture probability to vary over time (p has subscript t) and therefore deals with the important heterogeneity issue.

The challenge in applying the stratified Peterson estimate to Central Valley RST data, and in other systems, is that there may be no estimates of capture probability for some strata (that is no marks released, or no efficiency trial data), or the estimates may be very imprecise if few recaptures were obtained (either because not enough fish were released, or the capture probability was very low). This problem can be partially addressed through pooling, where some adjacent strata with no or limited data on capture probability are combined, and perhaps pooled with a stratum with more information (the Stratified Population Analysis System [SPAS] model developed by Arnason et al. 1996). The challenge here is that decisions on pooling can be somewhat arbitrary and can lead to unknown biases, which will underestimate uncertainty for the pooled strata. The approach is also time consuming to implement and different investigators may make different decisions about which strata to pool, resulting in inconsistent abundance estimates over years or across tributaries.

In the case of Central Valley RST data, as in many other systems, there are circumstances where some temporal strata are not sampled because trapping could not be conducted. There is no way to estimate abundance for these missing strata using the stratified Peterson estimator since there is no catch data (Equation 2).

Inferences about differences in abundance over years in a river system, or across systems, will be biased if there are substantial differences in the number of missing strata.

2.3 Bayesian Temporally Stratified Population Analysis System

Simon Bonner and Carl Schwarz developed BT-SPAS, a Bayesian approach to estimate capture probability and abundance from temporally stratified mark-recapture data. BT-SPAS addresses the limitations of the stratified Peterson estimator (Bonner 2008, Bonner and Schwarz 2011). BT-SPAS was initially developed to analyze RST data from the Trinity River in California (Schwarz et al. 2009), and is used in many systems, including the Stanislaus River (Pilger et al. 2019). BT-SPAS is a state-of-the-art method for analyzing RST data, and is available as an R library. We describe this model in some detail here, as its core elements are used in the model developed to estimate outmigrant abundance from Central Valley RST data, BT-SPAS-X, presented in Section 4.

We begin by providing a brief overview of Bayesian models (Section 2.3.1). We then describe the two fundamental components of BT-SPAS that predict capture probability (Section 2.3.2) and abundance (Section 2.3.3). We conclude with a discussion of the limitations of BT-SPAS in data-limited situations (Section 2.3.4). Readers familiar with Bayesian statistics, hierarchal models, and BT-SPAS can skip this section, as the structure of BT-SPAS-X is described in full in Section 4.

2.3.1 A Short Primer on Bayesian Modeling

The objective of Bayesian statistical models is to estimate the posterior probability distribution of a parameter (e.g., capture probability or abundance at RST site X in week t). The posterior distribution defines the probability for a range of parameter values given prior information about potential values, and information about parameter values from the data at hand. This is described by Bayes theorem, which can be simplified to:

Equation 3.

$$\mathrm{P}(a) \propto p(a) \cdot \mathrm{L}(data|a),$$

Where:

P(*a*) is the posterior probability of a parameter having a value of '*a,*' which is proportional to the product of p(*a*), the prior probability of value '*a,*' and

L(*data*|*a*), the likelihood of the observed data given a value of '*a.*'

The prior distribution is often based on information from other studies about the parameter. It is simply a statistical distribution (e.g., normal) that defines the probabilities over a range of parameter values. The likelihood is a measure of how well different values of the parameter fit the data the Bayesian model is applied to.

To provide a concrete example of Bayesian estimation, consider the estimation of capture probability (p) of an RST over a specific week based on r recaptures from R marked releases (efficiency trial data). The data likelihood computes the probability of a value of p (represented by 'a' in Equation 3) given data observations r and R. The prior probability could reflect our understanding of RST capture probability from other traps, or the trap in question in different time periods. In an ideal case, uninformative priors are typically used so that the data at hand defines the estimate. In this case one might assume that any value of capture probability between 0 and 1 is equally probable. This would be modeled by using a uniform distribution. An uninformative prior generally allows the data to completely determine the posterior probability. Alternatively, one might specify a more informative prior described by say a normal distribution with a mean of 0.1 and a variance σ^2. In this case the posterior will be influenced more substantively by the prior if σ^2 is low, implying there is more information in the prior distribution about the value of capture probability. The net effect of the prior and the data likelihood on the posterior depends on the relative differences in the amount of information about the parameter from these two sources. A modestly informative prior will have very little effect on the posterior if the amount of information about the parameter in the data likelihood is large. Conversely, a relatively uninformative prior can have an important influence on the posterior if there is very limited information about the parameter in the data.

In the simplest applications of Bayesian models, information from other studies is used to inform the prior distribution for the parameter of interest. The posterior is then estimated using this fixed prior distribution as well as the data specific to the study used in the data likelihood. However, in hierarchical Bayesian models (HBMs), both the prior and the posterior distributions for the parameter(s) of interest are jointly estimated. Consider the example where 10 efficiency trials are conducted over 10 weeks to estimate the weekly capture probabilities for an RST. This would result in 10 observations of recaptured marked fish $r_{t=1:10}$, from 10 different groups of released marked fish $R_{t=1:10}$. There are two obvious ways to use these data to estimate capture probability. The simplest approach would be to pool the data by summing r and R values across the 10 weekly trials, to calculate a single capture probability (p = sum(r)/sum(R)). Alternatively, capture probability could be calculated independently for each trial ($p_t = r_t/R_t$). The pooling approach assumes no variability in capture probability across trials, which could lead to substantial bias for trials that depart from the mean. However, the independent approach may result in very unreliable (imprecise) estimates of capture probability for trials where few recaptures are observed.

HBMs offer a useful alternative to address the pooled vs. independent estimation conundrum. HBMs jointly estimate the posterior and prior distributions. Using the RST capture probability example from above, the prior distribution represents the extent of variation in capture probability across the 10 weekly trials, while the data likelihood represents the fit of 10 different capture probabilities given the 10 observations of *r* and *R*. In HBMs, the prior distribution used to estimate the *p*'s for each trial is called a hyper-distribution. It represents the distribution from which the trial-specific *p*'s are assumed to have come from, and is defined by hyper-parameters, such as the mean and a variance for a normal distribution. If the data indicate there is little variation in *p*'s across trials, the variance of the hyper-distribution will be low, while the converse will be true if there is substantive variation in *p*'s. Relative differences in information about *p*'s from the hyper-distribution and the data determine the posterior distributions for the trial-specific *p*'s. For example, if one of the trials has limited information about *p* because few recaptures were observed, the *p* estimate will be more strongly influenced by the hyper-distribution. Conversely, differences in the extent of information about *p*'s in the data impact the estimates of hyper-parameter values. Trials with more information about *p* have a greater influence on hyper-parameters than trials with less information about *p*. In this example, the mean of the capture probability hyper-distribution is essentially an information-weighted mean from all 10 mark-recapture experiments. When estimating parameters of an HBM, there is no longer a need to define a prior for the parameter of interest (trial-specific capture probabilities). The hyper-parameters defining the hyper-distributions, which is the prior for the 10 capture probability estimates, are directly estimated. Instead, priors for the hyper-parameters must be defined.

A critical assumption in all HBMs is that the samples (say estimates of capture probability from 10 weekly trials) are random draws from a common distribution. Decisions on which observations arise from a common distribution must be made thoughtfully. For example, it might be reasonable to assume that capture probabilities from RSTs in tributaries of the Sacramento River come from a common distribution that describes the extent of variability across tributaries. On the other hand, it may not be reasonable to assume that capture probabilities from RST sites on the mainstem Sacramento River belong in the same hyper-distribution distribution used for tributaries. The much larger width and flow in the Sacramento River likely leads to lower capture probability compared to sites in tributaries. Thus, sites from tributaries and the mainstem would logically be assumed to arise from different hyper-distributions.

2.3.2 Capture Probability Estimation in BT-SPAS

In the equations that follow, variables beginning with Greek letters represent estimated parameters, bolded Roman letters represent data, and Roman subscripts represent indices.

Capture probability in BT-SPAS is estimated using an HBM. Here, each strata-specific (e.g., weekly) estimate of capture probability *within a trapping season* is assumed to be a random draw from a common distribution. This common distribution, referred to as a hyper-distribution, represents the variation in capture probability across strata during a trapping season (e.g., November of calendar year 2001 through May [inclusive] of calendar year 2002). Mathematically, this is described as:

Equation 4.

$$logit(p_t) \sim norm(\mu, \sigma^2),$$

Where:

μ is the mean of a normal hyper-distribution,

σ^2 is its variance, and

logit() indicates that the resulting draw of capture probability p is in logit space, and thus needs to be transformed prior to being used to estimate abundance.

The model is fit by jointly estimating the strata-specific capture probabilities p_t, and the hyper-parameters μ and σ. This is done using the following binomial data likelihood,

Equation 5.

$$r_t \sim bin(p_t, R_t),$$

Where:

~bin() indicates that the observed number of recaptures,

r_t is assumed to be a random draw from a binomial distribution with the probability of success equal to p_t, and

the number of trials equal to R_t.

This likelihood is the same as used to estimate the probability of obtaining say four heads (equivalent to r) based on 10 coin tosses (equivalent to R). If the coin was perfectly balanced, one would expect to obtain five heads on average, after conducting many trials of 10 coin tosses. But due to random factors, an observation of four heads from a single trial of 10 tosses would not be unexpected. The certainty in the estimate of p_t in this simple example would increase as the number of tosses is increased, just as certainty in capture probability would increase with the number of marks released. For a given number of coin tosses, certainty in the estimate of p_t will increase with the true value of p_t. For example, if 100 marked

fish are released, the certainty of the capture probability estimate will be much higher if the true p_t is 0.5, compared to 0.05.

The binomial likelihood properly accounts for sampling error from two-outcome experiments, such as the flip of a coin (that can only be a head or a tail), or an RST-based mark-recapture efficiency trial (a marked fish is either recaptured or not recaptured). Sampling error must be accounted for when estimating trial-specific capture probabilities and the hyper-parameters defining the distribution from which they arise. Owing to differences in the number of fish released among weeks, or differences in capture probability due to river conditions or other factors, the certainty (i.e., sampling error) in the capture probability estimates across weeks will differ. Logically, weeks with greater certainty in p should make a greater contribution to the hyper-parameters compared to weeks when p is less certain. The binomial likelihood appropriately weights each weekly capture probability estimate in the estimation of the hyper-parameters. Conversely, the hyper-distribution of capture probability can push-back on the weekly estimates. For example, if the mean capture probability across 20 weeks is 0.2, and there is very little variance across 19 of those weeks, a week with a capture probability of say 0.01 would be pulled toward the mean of 0.2, especially if there is substantive uncertainty in that particular estimate (e.g., because only 1 marked fish of 100 was recaptured). Here the HBM recognizes the high sampling error in the week with only one recapture, and shrinks the estimate of capture probability toward the mean of the hyper-distribution. However, if that estimate of 0.01 was more strongly supported, say because 100 marked fish were recaptured from 10,000 releases, there would be little shrinkage and instead the mean and the variance of hyper-distribution would change.

This HBM behavior is a very logical and common way of dealing with sparse or missing data, such as the limited and sometimes sparse efficiency trial data to estimate capture probability for Central Valley RSTs. HBMs are often described as partial-pooling method because they find a happy medium between a pooled estimate and independent estimates. In the RST context, the HBM approach will provide more reliable estimates of trial-specific capture probabilities when the data are sparse. Another significant advantage of the HBM approach in the RST context is that it can predict capture probability for strata when no mark-recapture data are available (e.g., R_t=0). In this case the estimated capture probability would be determined from random draws from the hyper-distribution. It is also possible to account for covariate effects on capture probability. For example, the mean of the hyper-distribution μ (Equation 4) could be predicted by the linear model:

Equation 6.

$$\mu_t = \mu_0 + \beta \cdot Q_t.$$

Here the mean of the hyper-distribution can be different for each weekly strata (μ_t), and is calculated based on an estimated intercept (μ_0, equivalent to μ in Equation 4) and an additive effect that is the product of a covariate value for that week, such as mean flow Q_t, and the estimated flow effect size, β.

2.3.3 Abundance Estimation in BT-SPAS

Estimates of abundance across strata based on the stratified Peterson model are assumed to be totally independent. That is, an estimate of abundance in week 't' in no way depends on abundance in weeks 't-1' or 't+1'. BT-SPAS does not assume that each strata-specific estimate is independent. It recognizes that temporal variation in abundance may follow a pattern, so that abundances in adjacent strata are more likely to be similar to each other than estimates separated by a longer period of time. This assumption results in better estimates of abundance in strata where data are sparse, and allows estimation of abundance in strata when no sampling is conducted.

The data likelihood for capture probability and abundance in BT-SPAS share the same form. The binomial likelihood used to estimate the abundance of unmarked fish is:

Equation 7.

$$u_t \sim dbin(p_t, U_t)$$

Returning to the coin flip example, u represents the number of heads obtained from U tosses, and p represents the probability of obtaining a head from a single coin flip. Unlike the example used for capture probability, the number of tosses (U) is unknown and is estimated given the observed number of heads (u) and an estimate of the probability of obtaining a head from a single coin toss (p) as determined by the capture probability model. This binomial likelihood will lead to more certainty in the unmarked abundance estimate U if capture probability is more certain. And even if capture probability is very precisely defined, abundance estimates will be more certain if capture probability is higher compared to if it is lower.

The stratified Peterson estimator assumes that the *U*'s in Equation 2 are completely independent. Thus, if an observation of u for a weekly stratum is missing, unmarked abundance cannot be determined. In addition, if capture probability is very low or highly uncertain, unmarked abundance will also be highly uncertain. The assumption of non-independence of *U*'s in BT-SPAS addresses these limitations. BT-SPAS uses a Bayesian penalized spline to predict *U*'s for each stratum. The predicted *U*'s are then used with the estimates of capture probability *p* from the HBM component of the model and compared to the observed unmarked catch *u* via Equation 7. The likelihood provides the information for BT-SPAS to

estimate the spline parameters predicting the *U*'s by fitting to the observations of unmarked catch.

A spline is simply a set of polynomials joined or 'splined' together at a series of knots (typically one knot for every four strata in a penalized spline application). A cubic spline is a third-order polynomial (i.e., y = a + b*x + c*x^2 + d*X^3). In common spline applications, the user defines a spline tension that specifies how quickly the spline parameters can change across knots. In the penalized spline case, the amount of information about variation in the dependent variable (U_ts in this case) determines the extent to which the spline parameters can vary. If there is high certainty in U_t estimates, and they vary substantially over adjacent strata, the spline will be more flexible and provide a good fit to the U_ts. However, if uncertainty in U_t estimates is higher, or if they are certain but do not vary much across strata, the spline will not let its parameters vary as much, so the spline will be stiffer and may not fit the U_ts as well compared to the former example case. Penalized splines essentially automatically tune the tension parameter that determines spline smoothness.

The Bayesian P-spline implemented in BT-SPAS uses a B-spline basis function to predict the log of unmarked abundance for each timestep:

Equation 8.

$$\log(U_t) = \sum_{k=1}^{K+q} \gamma_k \cdot \boldsymbol{B}_{\boldsymbol{k}(\boldsymbol{t})} + \nu_t \text{ I(,20)}$$

Where:

q is the order of the polynomial (q=3 for the cubic spline used in BT-SPAS),

k defines the index for each knot, and

K is the total number of knots. B is a pre-computed basis function that defines the contribution of each spline parameter γ for each strata t.

ν_t is an extra-spline deviate drawn from a normal distribution with means predicted by the spline estimates for each timestep 't'.

I(,20) limits the maximum value of predicted log abundance for each timestep to 20 (approximately 485 million).

BT-SPAS assumes that the prior distributions of spline parameters vary according to a second order random walk:

Equation 9.

$$\gamma_{k+1} - \gamma_k = b\gamma_k - \gamma_{k-1} + \delta_k,$$

Where:

δ_k is a normally-distributed random variable with mean 0 and variance σ_U^2.

Put more simply, the difference in adjacent spline coefficients at knots k and k+1 is assumed to be related to the difference between values at k-1 and k. The extent of similarity depends on the magnitude of the random normal deviate. If the deviates are large, because σ_U^2 is large, the spline parameters can vary substantially across knots, and the spline will be flexible. Conversely, if σ_U^2 is small, then the deviates will be smaller, spline parameters will vary less, and the spline will be stiffer. The certainty in U_t and its variability across strata determine the magnitude of the σ_U^2 estimate.

Patterns in outmigrant abundance over strata may follow a general shape that can be well approximated by a spline. However, it is also possible that there are sudden increases or decreases in outmigrant abundance across weeks due random factors, or known factors such as a sudden increase in flow following a prolonged period of low flow. In these cases, the spline would not fit the estimates of U_t near the rapid transitions very well. To account for this issue, BT-SPAS estimates the extent of extra-spline variation σ_{Ue}^2 to predict extra-spline deviates for each stratum. If there is strong evidence for considerable extra-spline variation, the estimate of σ_{Ue}^2 will be large and hence v_t values will be large for some strata.

The penalized spline approach adopted in BT-SPAS is flexible in that model complexity is automatically adjusted based on the amount of information in the data. In statistics, models with more parameters are considered more complex. These models will typically exhibit low bias, but may be imprecise in information-poor situations because some parameters will be poorly defined if they do not have a large influence on fit. Conversely, models with fewer parameters are considered simpler and will make more precise predictions, but have the potential to be more biased. Information theoretic approaches, like the familiar Akaike Information Criteria (AIC), quantify the trade-off between bias and precision given the data at hand. AIC can be used to identify a level of model complexity that strikes the best balance between bias and precision, and therefore has the best predictive ability. However, using an AIC-like approach requires testing a series of increasingly complex models. BT-SPAS automatically adjusts model complexity via σ_U^2 and σ_{Ue}^2, based on the information in the data about variation in U_t. Fits that result in more flexible splines, or with higher extra-spline variation, resulting from more certain estimates of U_t and extensive variation in U_t's across strata, represent a more complex model. This approach estimates the optimal model complexity without any user intervention.

2.3.4 BT-SPAS Limitations

There are a few important limitations in BT-SPAS worth discussing in the context of Central Valley RST data. First, the spline approach in BT-SPAS can make poor predictions for strata when the trap was not operated, especially when capture probability is uncertain. This leads to greater uncertainty in estimates of strata-specific abundances that can lead to unreasonably high abundance estimates in some cases. Second, the HBM approach used to estimate capture probability in BT-SPAS requires a reasonable number (approximately 10) of informative efficiency trials within a trapping season. It does not consider efficiency trial data from other years in the estimation of capture probability for weeks within in a specific run year. If there are too few trials for a trapping season of interest, or if most trials contain little information about capture probability (e.g., because few recaptures were observed), the model will struggle to estimate the hyper-parameters for the capture probability hyper-distribution. For most Central Valley RST locations, the majority of tributary and run years do not have a sufficient number of efficiency trials to estimate the capture probability hyper-distribution. This data limitation will be discussed more fully in the next section of this chapter. As a result of this data limitation, a modified version of BT-SPAS (BT-SPAS-X) was developed to analyze the Central Valley RST data.

There are a few related issues in the BT-SPAS documentation (Bonner and Schwarz 2011) and source code[1] worth reviewing in the context of the HBM and spline model limitations identified above.

2.3.4.1 Missing Strata

Oddly, BT-SPAS includes strata with no data in the likelihood computation for weekly abundance estimates (Equation 7). To do this, unmarked catch is set to 0 and a very low capture probability is assigned to the stratum. This approach effectively creates a prior on the upper limit of abundance in these strata, since increasingly large estimates of abundance are increasingly penalized (a catch of zero would be unlikely at very high abundance even under the assumed very low capture probability). This prior is both unintuitive and illogical. For strata that were not sampled, the capture probability is unequivocally zero, and since there is no catch data, there is no information about abundance based on data for the stratum. A logical and more straightforward approach that is adopted in BT-SPAS-X, is not assume catch is zero for unsampled weeks, and instead use an upper limit on abundance for problematic strata. BT-SPAS also uses an upper limit on abundance, which is not user-defined but instead hard-wired in the code as 20 in log space

[1] https://github.com/cschwarz-stat-sfu-ca/BTSPAS/blob/master/R/TimeStratPetersenDiagError.R

(485 million). The very large prior on maximum abundance is not sufficient when there is high uncertainty in capture probability.

2.3.4.2 Calculation of Capture Probability

A questionable formula is used to calculate the logit of capture probability for each stratum in the BT-SPAS source code. The description of the model code (Bonner and Schwarz 2011) indicates that the logit of capture probabilities is based on random draws from a normal distribution. The mean for that hyper-distribution is reported to be calculated solely from an estimated intercept and covariate effects if specified by the user. However, examination of the source code (line 138 of code specified in footnote) shows the strata-specific capture probability estimates are adjusted based on the ratio of unmarked catch to estimated abundance. The comment above the code is " `## Matt's fix to improve mixing. Use u2copy to break the cycle (this doesn't work??)`". Our limited understanding of the logic here is that capture probability is logically informed by both r/R (recaptures/marked releases) and u/U (unmarked catch to estimated unmarked abundance), and including the latter somehow improves estimation properties.

The revised version of BT-SPAS we developed for Central Valley RST data does not include this questionable adjustment in the capture probability computation, and does not include missing strata in the data likelihood for capture probability. We use a more direct approach where an upper limit on abundance for each model week is specified as a constraint.

3 Summary of Central Valley RST Data

A summary of the compiled data from Central Valley RST sites is provided here to rationalize the need to modify BT-SPAS to account for limitations in the Central Valley data.

Daily unmarked catch, and the daily number of marked fish that were released and recaptured (efficiency trials) were aggregated into weekly strata. Examination of daily recaptures showed that the vast majority of marked fish were recaptured within a few days from release, and it was very rare for a recapture to occur more than one week after release. Weekly values were organized into run years so that the model could estimate abundance for each trapping season. Data from weeks in November and December in calendar year 't-1' were assigned the same run year as weeks from January through end of May in calendar year 't' (for run year 't'). This is very similar to water year assignments, which group discharges from October through December from one calendar year with discharges from January through September in the next calendar year.

To apply BT-SPAS-X, the weeks to include for each run year must be defined. If modeling abundance from November 4 in year t-1 to May 27 in year t, the model would estimate abundance for 31 weeks. The model does not require that catch is observed for each of these weeks because it can interpolate abundance for a limited number of missing weeks. A total of 170 years of data are available across 15 sites in our Central Valley RST data set for tributaries of the Sacramento River (Table 1). Some sites, such as upper Battle Creek, Butte Creek, upper Clear Creek and lower Clear Creek, have been sampled for approximately 20 years or more. We anticipate that an iterative process is needed to inform the decision on the optimal run year window and the minimal number of sampled weeks within that window necessary to include a run year in the modeled dataset for JPE model. A wide window (e.g., October–June) would include all of the outmigrating spring-run juvenile abundance for the year based on run periods defined by Cordoleani et al. (2021). However, the wider the window, the greater number of years with missing weeks at the start or end of the trapping season. A more truncated trapping season (e.g., the November through May period) would reduce the number of missing weeks at the edges of the season and would require less influential priors.

We compiled an extensive dataset of trap efficiency, with a total of 1,056 efficiency trials from 14 RST sites (Table 2, Figure 1). The number of trap efficiency trials within sites was highly variable, ranging from approximately 100–200 for intensively sampled sites (Battle Creek, upper and lower Clear Creek, Eye Riffle, Steep Riffle, and Herringer Riffle on the Feather River), to more modest numbers of approximately 10–20, generally from sites where trap efficiency trials only began in recent years (e.g., sites at Butte, Deer and Mill creeks). In most cases the sample size of efficiency trials within site and run years was small. For example, Battle

Creek has a total of 131 mark-recapture experiments across 18 run years. However, the median number of experiments within a run year was only six, an insufficient number for a successful implementation of BT-SPAS, which only considers within-year efficiency trials in the estimation.

The expectation of capture probability for each efficiency trial ($p_t=r_t/R_t$) were plotted for each RST site as a function of the number of marks released (Figure 2). There is no reason to expect that capture probability will vary as a function of the number of fish released. However, the certainty in the capture probability estimate will increase with the number of marked fish released at a given capture probability. We calculated the uncertainty in capture probability based on the number of marked fish released (R) and capture probability (p) using the standard binomial formula for relative variation in the number of recaptures:

Equation 10.

$$cv = \sqrt{\frac{1-p}{R \cdot p}},$$

Where:

cv is the coefficient of variation in the estimate of capture probability.

A smaller cv indicates greater precision in the estimate of capture probability, which in turn reduces uncertainty in capture probability and abundance parameters in our model. This equation demonstrates that precision in capture probability estimates increases (i.e., cv decreases) with the number of marked fish released or with capture probability, because an increase in either of these would result in a higher number of recaptures. Thus, experiments conducted when capture probability is high, and when many marks are released will have a higher number of recaptures and higher precision (that is low cv values, upper-right quadrant of panels in Figure 2), while experiments conducted when capture probability is low and when few marks are released will have lower precision (lower-left quadrant). The square root component of the Equation 10 indicates that there is a non-linear decrease in precision as R or p values become smaller. Conversely, increases in R or p have diminishingly positive effects on precision. This is why the spacing of the red precision lines in Figure 2 increases when moving from the low-precision corner of the plot (lower left) to the high-precision corner (upper right).

Figure 2 can be used by stream teams to make decisions on how many marked fish to release for an efficiency trial to attain a target precision. The black horizontal lines in the plots show the average capture probability for each site. Investigators can use the contours to achieve at target precision of capture probability for an efficiency trial. For example, to achieve a target precision of cv = 0.1 under the typical capture probability at the Battle Creek RST site, about 3,000 marked fish

must be released, while about 1,000 marked fish will achieve a precision of 0.25. Note the diminishing returns to precision with increases in the number of marks released as one works rightward on the x-axis. The majority of mark-recapture experiments from RST sites in Sacramento River tributaries yielded relatively precise estimates of capture probability (Table 3). For example, 76% of the 131 trials in Battle Creek had a *cv* equal to or less than 0.25. In contrast, most sites with very low trap efficiency and/or with a low number of releases (Deer Creek, Yuba River, Live Oak and Lower Feather sites on the Feather River) had low proportions of high-precision efficiency trials.

4 BT-SPAS-X: A Modified Version of BT-SPAS to Address Data Limitations in Central Valley RST Data

We developed a modified version of BT-SPAS, hereafter referred to as BT-SPAS-X, to estimate the abundance of outmigrant juvenile Chinook salmon at RSTs in tributaries of the Sacramento River in California's Central Valley (Figure 1). The revised model addresses unique data limitations in Central Valley RST data. Like BT-SPAS, there are two major components of BT-SPAS-X. An HBM is used to estimate capture probability for each weekly strata (Section 4.1), and a Bayesian penalized spline model is used to estimate abundance given the catch of unmarked fish and estimates of capture probability (Section 4.2).

In the equations that follow, variables beginning with Greek letters represent estimated parameters, bolded Roman letters represent data, and Roman subscripts represent indices of the variables (e.g., model week 't').

4.1 Capture Probability

4.1.1 Estimation

The capture probability component of BT-SPAS-X jointly estimates the capture probabilities for all sites, years, and weeks by fitting the model to all available RST mark-recapture data (efficiency trials) from Sacramento River tributaries. Like BT-SPAS, it uses a hierarchical Bayesian modeling approach. Capture probability (p) at RST site 's' in year 'y' on week 'w' is predicted by:

Equation 11a.

$$logit(p_{s,y,w}) = \beta\_S_s + \beta\_Q_s \cdot \boldsymbol{Q_{s,y,w}} + \varepsilon_{s,y,w},$$

Equation 11b.

$$\varepsilon_{s,y,w} \sim dnorm(0, \sigma_P)$$

Where:

logit indicates that capture probability is estimated in logit space,

β_S are estimated intercepts for each site s,

β_Q are estimated effects of flow on capture probability for each site,

Q is the average standardized flow for each site for year y and week w, and

ε is a random effect drawn from a normal distribution with standard deviation σ_p. σ_p represents the amount of variation in capture probability not explained by the fixed effect β terms.

This is the unexplained variation that will also be referred to as process error. The ε terms are random effects that account for limitations of model structure to explain the variance of the data (Barry et al. 2003). For example, the effect of flow on capture probability may be different for weeks early in the run year compared to later in the year. The use of random effects also avoids negative bias in variance estimates resulting from pseudo-replication (Millar and Anderson 2004).

The parameter β_S predicts the extent of variation in the mean capture probability among RST sites. The parameter β_Q predicts the effect of flow on capture probability, and this effect is also allowed to vary across sites (hence the 's' subscript). Flow values (***Q***) were centered and standardized by subtracting the mean flow for the site across all years and weeks included in the estimation, and then dividing by the standard deviation of all these weekly flow values. Thus, if flow for a week was equal to the average value across all years and weeks, the standardized value of *Q* is zero, and the average capture probability at site s is determined only by β_S_s and the random effect, because the product of $\beta\_Q_s \cdot \boldsymbol{Q}$ would be zero. Note that because flow was standardized to mean flow *within* each site, rather than mean flow *across* all sites combined, the flow covariate effect modifies capture probability based on variation in flow only *within* an RST site, and does not predict variation in capture probability across sites. Therefore, differences in capture probability at the mean flow for the site for each site is solely determined by β_S_s.

Site-specific intercepts (β_S) and flow effects (β_Q) in the capture probability model are assumed to come from common normal hyper-distributions:

Equation 12a.

$$\beta\_S_s \sim dnorm(\mu_S, \sigma_s)$$

Equation 12b.

$$\beta\_Q_s \sim dnorm(\mu_Q, \sigma_Q)$$

Where:

the μ's represent the estimated across-site means of the hyper-distributions, and

the σ's represent their estimated standard deviations.

We use uninformative normal prior distributions for the μ's (mean 0 and variance of 1E06) and uninformative gamma distributions for the precision (1/variance) of the distributions, which are then converted to priors for the σ's. The partial pooling created by the hierarchical structure of the site and flow effects provide better predictions of β_S and β_Q estimates compared to models that assume these parameters do not vary across sites (fully pooled), or that assume site-specific parameters are completely independent of each other. With this modeling structure, sampling from the hyper-distributions provides a logical way to account for the additional uncertainty in estimates of capture probability for tributaries without any efficiency trial data. Conversely, the hierarchical approach can improve precision at sites with few trap efficiency trials.

The capture probability model was fit to the RST efficiency data using a binomial data likelihood:

Equation 13.

$$r_{s,y,w} \sim binomial(p_{s,y,w}, R_{s,y,w})$$

Where:

r is the observed number of marked fish that were recaptured, and

R is the number of marked fish that were released.

The terms of the capture probability model (Equations 11 and 12) were estimated by applying the model to all weekly observations of releases and recaptures across 14 RST sites in Sacramento River tributaries that had efficiency trial data (refer to Table 3). Estimated site, year, and week deviates ($\varepsilon_{s,y,w}$) varied across observations to provide a near perfect fit to the data (i.e., p values close to *r*/*R*). The deviates can be thought of as residuals that are approximately the difference between the observations of capture probability (*r*/*R*) and what was predicted by the β_S, and β_Q effects in the capture probability model (Equation 11). In simple linear regression, the residuals are computed after the effects are calculated, and the residual variance is then calculated from these values. Because we used a hierarchical model, the deviates, called random effects, are jointly estimated along with variance of the normal distribution that generates them, as well the other parameters in the model. The model maximizes the posterior probability by explaining as much of the variation in capture probability observations based on β_S, and β_Q, and then picks up much of the remainder of the variation with the ε terms.

The data likelihood to fit the capture probability observations (Equation 13) accounts for differences in the amount of information across-site, year, and weekly strata. Strata with a more recaptures have more information about capture probability. As a result, the model fit relied more on these observations compared

to those from strata with less information about capture probability (i.e., strata in which few recaptures were observed).

4.1.2 Applying the Model to Strata with no Efficiency Trial Mark-recapture Data

The capture probability model in BT-SPAS-X can be used to predict capture probability in weeks when no efficiency trial data available. For RST sites with some trap efficiency data, the model predicts capture probability using site-specific estimates of β_S and β_Q, the value for Q for the year and week being estimated, and a random draw of an ε deviate from Equation 11b. If the unexplained process error for the capture probability model (σ_p) is high, the additional uncertainty associated with the random ε draw will be considerable. As a result, the uncertainty in capture probability for a week with no efficiency data will be much higher compared a week with mark-recapture data. In the latter case, the ε deviate is much better defined and so capture probability is more certain.

The capture probability model can also be applied to RST sites that have no efficiency data at all. In this case, random draws of β_S and β_Q from their hyper-distributions (Equations 12a and 12b) are taken, and the approach described in the previous paragraph is then implemented. Capture probabilities will be more uncertain in this case because of the additional variance introduced through the random draws of β_S and β_Q from their hyper-distributions.

The key difference between BT-SPAS and BT-SPAS-X with respect to capture probability is that BT-SPAS-X jointly estimates it for all RST sites, trapping seasons (run years), and weeks within each trapping season. In contrast, BT-SPAS estimates weekly capture probabilities for each run year and site individually. By jointly fitting to all the mark-recapture data, BT-SPAS-X makes more reliable predictions of capture probability for sites with only limited number of efficiency trials within a run year (Table 2). The model essentially borrows information from all run years and weeks where efficiency trials were conducted, to estimate the capture probability each particular, site, run year, and week. The structure of the capture probability model presented here (Equation 11) can be modified in the future, by adding covariates, to produce more reliable predictions. As will be shown below, there is strong statistical support for capture probability models that includes effects of RST site and flow. Other effects can easily be added to the model and used to predict abundance if there is statistical support for them.

4.2 Chinook Salmon Abundance (All Run Types)

4.2.1 The Spline Model

BT-SPAS-X estimates abundance for weekly strata based on the catch of all run types of Chinook salmon using a Bayesian penalized spline model. This is the same approach as BT-SPAS, but with the addition of a covariate effect to explain some of the variation in abundance over weeks. The model predicting the log of unmarked abundance in model week *t* is:

Equation 13.

$$\log(U_t) = \sum_{k=1}^{K+q} \gamma_k \cdot \boldsymbol{B}_{\mathbf{k(t)}} + \phi \cdot \boldsymbol{X}_{\mathbf{s,y,w}} + \nu_t \; T(, \lg N\_max_t),$$

Where:

q is the order of the polynomial (*q* = 3 for the cubic spline used in this application),

k defines the index for each knot,

K is the total number of knots (one knot per four strata), and

t is an index for the weekly strata for the RST site and year that the model is applied to.

B is a pre-computed basis function that defines the contribution of each spline parameter γ to the prediction of abundance for each weekly stratum. ϕ is an estimated effect that allows extra-spline variation in abundance to vary as a linear function of covariate value ***X*** (e.g., flow). ν_t is a deviate that allows random extra variation in abundance beyond what is predicted by the spline and covariate effects, and will be described in more detail below. The log of unmarked abundance is estimated in units of 1,000 for numerical precision, and converted to unlogged units prior to use in the data likelihood (Equation 13). The T(, lgN_max$_t$) term limits predicted abundance to a value no greater than lgN_max$_t$. This constraint can be set to a very high value so it has no effect on predictions, or a lower value for specific strata to constrain unrealistically high values resulting from sparse data.

The model predicting the log of abundance by weekly strata (Equation 13) is the same as in BT-SPAS except for the addition of a covariate effect ($\phi \cdot \boldsymbol{X}_{\mathbf{s,y,w}}$). The spline component of the prediction can be thought of as the intercept in a simpler linear model. But rather than being a constant, it can vary in a smooth way across weekly strata. The covariate effect allows the predicted weekly estimated log of abundances to vary in a structured way around the spline-predicted intercepts based on the covariate values. The covariate effect was added to test the

hypotheses that occasional increases in flow can lead to an increase in outmigration abundance. If this is the case, we would expect to see a positive estimate for ϕ. Note covariate values *X* could represent the within-tributary standardized average weekly flow, or a derived variable, such as the difference in flow from the previous week. Another alternative is to make *X* an indicator variable, taking on values of 0 or 1 if the relative flow increase is less than or greater than a specified threshold, respectively. The current version of BT-SPAS-X does not include the $\phi \cdot \boldsymbol{X}_{\mathbf{s,y,w}}$ element in Equation 13.

We assume that the prior distributions of spline parameters γ vary according to a second order random walk:

Equation 14a.

$$\gamma_{k+1} - \gamma_k = \gamma_k - \gamma_{k-1} + \delta_k \text{ for k=2:K,}$$

Equation 14b.

$$\delta_k \sim dnorm(0, \sigma_U)$$

Equation 14c.

$$\gamma_{k=1:2} \sim dflat()$$

Where:

δ_k is a normally-distributed random variable with mean 0 and standard deviation σ_U.

Put more simply, the difference in adjacent spline parameters from knot k to k+1 is assumed to be related to the difference between values k-1 and k. The extent of the difference depends on the magnitude of the random normal deviates δ_k. If the deviates are large, because σ_U is large, the spline parameters can vary substantially across knots, and the spline will be flexible. Conversely, if σ_U is small, then the deviates will be smaller and spline parameters will vary less and the spline will be stiffer. The certainty in U_t and its variability across strata determine the magnitude of the σ_U estimate. Different priors for spline coefficients are needed for the fist two values of k. BT-SPAS uses a flat prior for k = 1 and 2. A flat prior predicts the same prior probabilities for all values of γ_1 and γ_2.

Patterns in outmigrant abundance over strata may follow a general shape that can be well approximated by a spline and perhaps even covariate effects such as flow. However, it is also possible that there are sudden increases or decreases in outmigrant abundance due random factors not accounted for in the abundance equation. In these cases, the spline and covariate effects would not fit the estimates of U_t well. To account for this possibility, extra-spline deviates for each

stratum, ν_t, are drawn from a normal distribution with estimated standard deviation σ_{Ue}:

Equation 15.

$$\nu_t \sim dnorm(\mu_{Ut}, \sigma_{Ue})$$

Where:

μ_{Ut} is the prediction from Equation 13 excluding ν_t values.

If there is strong evidence for considerable extra-spline variation based on the pattern of U_t values, the estimate of σ_{Ue} will be larger to allow ν_t values to be more variable across strata. Although σ_{Ue} is sometimes referred to by the term "extra-spline variation," this term is only accurate if the covariate effect in Equation 13 is not estimated. If a covariate effect is estimated, σ_{Ue} is more accurately defined as the "additional variation" not explained by both the spline and covariate effects. However, for brevity we use the term "extra-spline variation" for both cases. Like BT-SPAS, BT-SPAS-X uses uninformative gamma priors for the inverse of spline and extra-spline variances,

Equation 16a.

$$\sigma_U^{-2} \sim dgamma(1, 0.05)$$

Equation 16b.

$$\sigma_{Ue}^{-2} \sim dgamma(1, 0.05)$$

Parameter values that predict abundance (Equation 13) are estimated by comparing the abundance estimates to the catch data given the estimates of capture probability using:

Equation 17.

$$u_t \sim dbin(\pi_t, U_t)$$

Where:

π are weekly estimates of capture probability generated from Equation 18 below.

Note that values of u_t are adjusted to account for differences in trapping effort prior to running the model. To do this, the average number of hours a trap is fished each week (effort) over the modeled period (e.g., November–May) is computed for all run years for the tributary being modeled. If more than one trap is fished the sum of hours across both traps is used in computing the average. The adjust weekly

catch is calculated as the product of the observed weekly catch and the ratio of the weekly effort (hours fished over week) to the average effort.

Capture probabilities (π_t) used in the abundance model are estimated from:

Equation 18.

$$logit(\pi_t) \sim dnorm(\boldsymbol{\mu}_{\boldsymbol{p}_t}, \boldsymbol{\sigma}_{\boldsymbol{p}_t})$$

Where:

μ and σ terms are the weekly mean and standard deviation of weekly capture probabilities in logit space estimated from the posterior distributions of logit-transformed capture probability estimates generated by the capture probability model (Figure 3).

Note μ and σ are treated as data in the abundance model (Figure 3). We use the cut() function in the Bayesian inference using Gibbs sampling (BUGS) modeling software so that predictions of π are not influenced by the fitting of u (unmarked catch) in the abundance model.

4.3 Estimation of Spring-run Chinook Salmon Abundance

A PLAD model (Chapter 6) is used to convert weekly estimates of total Chinook salmon abundance for any site and run year (Section 4-2) into estimates of spring-run abundance (srU_t) using,

Equation 19.

$$srU_t = U_t \cdot srP_t$$

Where:

srP_t is the PLAD-based estimate of the spring-run proportion in week *t*.

The PLAD estimates of srP_t are fit to site-specific genetic data and the length frequency of the RST catch in each week. To date, PLAD results from Sacramento River tributaries are available for RST sites at Battle Creek, upper and lower Clear Creek, Mill Creek, Deer Creek, Butte Creek, and Yuba River (Figure 1). Additional work (in progress) is needed to apply the model to RST sites on the Feather River (refer to the discussion of Feather River in Chapter 3).

4.4 Estimation

The model estimates the parameters that predict weekly abundance of Chinook salmon U_t for all weeks for a given RST site and run year. The model is run in three parts. First, the capture probability component of the model is run (Figure 3). This model estimates capture probability for all weekly efficiency trials from all RST sites and the hyper-parameters from which they are calculated. Second, the posterior distributions of these parameters are passed to an R script to calculate capture probability for each week of the site-run year being modeled. Finally, the means and standard deviations of weekly capture probabilities generated from the script are read-in by the abundance component of the model to estimate weekly and annual abundance. This approach ensures that the abundance component of the model does not influence the parameters determining capture probability (hence the red triangle in Figure 3). Thus, capture probability parameters that determine weekly values for any site and run year will be the same for all site and run year cases.

Posterior distributions of the capture probability model were estimated using stan statistical software (version 3.35.0; Stan Development Team 2024) called from the rstan library (version 2.35.0) from R (version 4.4.1; R Core Team 2024). Posterior distributions were based on 10,000 simulations per chain. Convergence was evaluated based on Gelman and Rubin's (1992) scale reduction factor. Weekly and annual abundance were estimated using the BUGS software (Spiegelhalter et al. 1999) called from the R2WinBUGS (Sturtz et al. 2005) library. BUGS was used because it contains a cut() function that does not allow estimates of abundance to influence weekly capture probability values. Posterior distributions were based on taking every second sample from each of three chains from a total of 2,000 simulations per chain, after excluding the first 500 burn-in samples to remove the effects of initial values. These sampling characteristics were sufficient to achieve adequate model convergence as evaluated using the Gleman and Rubin scale reduction factor.

The model was applied to weekly catch data for Chinook salmon of all run types if designated as a fry or smolt life stage. Estimates of the spring-run proportion for each RST site, run year, and week, derived from the PLAD model, were multiplied by the total Chinook salmon weekly abundance estimates from BT-SPAS-X to estimate the abundance of spring-run (Equation 18). To do this, each posterior sample of weekly total Chinook salmon abundance was multiplied by a random sample from the posterior distribution of the spring-run proportion from PLAD in that week. Thus, the calculation of weekly spring-run abundance accounts for uncertainty in the PLAD-based spring-run proportions. Weekly PLAD predictions are made based on the size distribution of fry only, smolts only, or the combined size distributions. As this chapter uses the combined catch of weekly fry and smolt counts, we used the combined PLAD predictions.

5 Application of BT-SPAS-X to Estimate Capture Probability and Outmigrant Abundance in Sacramento River Tributaries

5.1 Data Used in Modeling

For the purposes of this review, we modeled an outmigration period of November 4 through May 27 (31 weeks). BT-SPAS-X was applied to data from 170 run years across 15 RST sites (Table 1, Figure 1).

5.2 Capture Probability Model Results

Predictions of 1,056 trap efficiencies from Equation 11 fit the observed capture probabilities (r/R) very well (r^2=0.99). The excellent fit occurred because the capture probability model estimates efficiency trial-specific random effect deviates. Parameter estimates from the model indicate substantial variation in capture probability among sites and with flow. The transformed mean of the hyper-distribution for site effects (μ_S) was 0.025 (Figure 4a). The mean estimates of β_S (closed points) were generally very close to the expected capture probabilities for each site (open points), calculated by taking the ratio of the sum of recaptures and releases across all efficiency trials within each site (i.e., the expected values). There was evidence for modest statistical shrinkage toward the mean for Butte Creek and the Steep Riffle site on the Feather River. These sites had unusually high trap efficiencies compared to the majority of others due to unique trapping conditions. These sites may therefore not be statistically exchangeable with the others, a key assumption with the hierarchical modeling approach in BT-SPAS-X. Abundance estimates at these two sites could be overestimated in some years because capture probabilities could be underestimated. We therefore implemented an alternate structure where we assumed the mean capture probabilities for these sites (β_S) are independent (not exchangeable), rather than random variables drawn from a common hyper-distribution (Figure 4b). This change led to a narrower hyper-distribution and better alignment of expected (blue points) and modeled (black points) estimates for the two non-exchangeable sites.

There was evidence for a negative effect of discharge on capture probability for some of the RST sites with trap efficiency data (Figure 5a). In a few cases (at Battle Creek, upper and lower Clear Creek, Mill Creek, and Herringer Riffle site on the Feather River) trap efficiencies were measured across a wide range of flows, providing a relatively convincing pattern of effect. However, in most cases trap efficiencies were mostly measured at a discharge near the mean, providing insufficient contrast in flow across efficiency trials to reliably estimate a flow effect. The hyper-distribution of the flow effect, estimated largely from the more

informative sites, dominated the site-specific flow effect estimates for sites without an adequate range of flows. Results for Butte Creek provide an illustrative example. When the prior for flow slope for this site (and Steep Riffle on the Feather River) was based on the hyper-distribution, the effect of flow on capture probability was negative (Figure 5a). In contrast, when these sites were considered non-exchangeable with the others, the flow slope was positive and considerably more uncertain (Figure 5b).

We examined the effect of fish size on capture probability. To do this, the dataset was trimmed from 1,056 to 467 records where average fork length of fish released in efficiency trials was recorded (Figure 6). Surprisingly, there was no apparent effect of fish size on capture probability. Owing to the reduction in sample size if modeling a fish size effect, and this pattern, we did not test a model that include a fish size effect on capture probability.

Capture probabilities for hatchery-origin releases in efficiency trials were approximately 50% lower than those based on releases of natural-origin fish (Figure 7). However, the origin of releases was only recorded for 91 of 1,056 trap efficiency trials. The majority of trials where origin was recorded (86) came from only one site (Battle Creek). A potential effect of fish size on capture probability could confound effects of origin. However, this did not appear to be the cases as smaller hatchery-origin fish released at Battle Creek had lower capture probability compared to natural-origin fish of approximately the same size range. Owing to the limited sample size for trap efficiency data where origin was specified, we did not include origin as an effect in the capture probability model.

5.3 Capture Probability and Abundance Estimates by Run Year

We examined model predictions of weekly capture probability and abundance for a select set of RST sites and run years. The intent is to demonstrate critical aspects of model behavior under data-rich and data-poor conditions. Model predictions are compared to stratified Peterson estimates in weeks when mark-recapture data are available. The majority of results are based on the combined catch of all juvenile (fry and smolt life stages) Chinook salmon run types. Predictions of spring-run abundance require additional calculations using estimates of spring-run proportions from the PLAD model, which is currently only available for a single site and run years. Thus, this chapter focuses on abundance predictions across all run types, but provides predictions of spring-run abundance for a single case where the PLAD model to demonstrate the approach.

Results presented here are based on a prior that sets an upper limit on the log of predicted weekly unmarked abundance (lgN_max in Equation 13). For any RST site and run year, the weekly priors are calculated from:

Equation 20.

$$\text{lgN\_max}_t = \log\left(\frac{(u_t + 1) \cdot 0.001}{0.005}\right)$$

The unmarked catch for each stratum was converted to units of thousands and divided by an assumed minimum capture probability (0.005, 0.5%), and then converted to log space. The average of lgN_max over a trapping season in a given run year was used to calculate the abundance constraint for weeks that were not sampled (i.e., when observations of u_t were not available). This is a simple rule that is easy to modify. BT_SPAS uses a constant maximum constraint on log abundance of 20. The approach adopted BT-SPAS-X (Equation 20) allows this constraint to vary over sites and weekly strata.

The 2008 run year for Battle Creek is a relatively data-rich case with trap efficiency data for 16 of 31 strata (Figure 8a, Table 2). Model predictions of capture probability in these strata (grey bars in bottom panel) matched the Peterson estimates (open blue points) very well. Small discrepancies occurred when there was limited information in the efficiency data, such as when 4 of 254 marked fish were recaptured in the week starting Dec-23. The *r*/*R* Peterson estimate (4/254) is uncertain for this stratum owing to the low number of recoveries, so the model pulled the estimate upwards toward the expectation predicted by the capture probability model given the estimated site and flow effects. In weekly strata without efficiency data, model predictions were solely driven by capture probability parameters (Equation 11a) and random draws of process error deviates (Equation 11b, red bars in Figure 8a). Logically, this resulted in considerably wider 95% credible intervals for both capture probability and abundance estimates relative to strata with informative efficiency trial data. The variation in the height of the red bars for capture probability across strata (indicating a lack of efficiency trial data) was driven by predicted flow effects, with lower capture probability when flows were high, and visa-versa (Figure 5). More discharge-driven variation in capture probability would be seen in run years with greater variation in flow across weeks, or at sites where flow effects were stronger. As expected, capture probability was less certain for periods without efficiency trial data (e.g., December 30), which resulted in greater uncertainty in weekly abundance estimates, and was more certain for periods with efficiency trial data (e.g., December 23).

Weekly abundance estimates from BT-SPAS-X fit the Peterson estimates very well for the Battle Creek 2008 run year. Uncertainty in the total abundance estimate for the run year depended on the number of efficiency trials and the degree of overlap in weeks with efficiency data and high catch. For example, the relative variation in the abundance estimate for run year 2017 at Battle Creek was relatively high (Figure 8b, CV = 36%). This occurred because there were only four weeks with efficiency data and they occurred in weeks with relatively low catches. As a result,

the uncertainty in capture probability for weeks with high catch was higher, resulting in greater uncertainty in the annual estimate. Contrast this situation with Battle Creek in 2008, which had a relatively precise annual estimate (CV = 20%) because there were many more weeks with efficiency data, and almost all weeks with high catch had efficiency data (Figure 8a).

Statistical shrinkage in capture probability estimates in weeks with efficiency trial data had have substantive effects on weekly abundance estimates. Consider estimates for lower Clear Creek for run year 2007 (Figure 8c). There were only three recaptures from 389 releases in the week beginning February 12. Note that the point estimate of capture probability (r/R) was less than half of the model-based estimate. The model shrunk capture probability toward the mean because there was very little information in the data owing to the low number of recaptures, and because the point estimate was unusually low for this site given the discharge. As a result of the higher capture probability from the model, the model-based estimate of abundance was considerably lower than the point estimate.

Estimates from lower Clear Creek in 2008 show model predictions for a case with lots of information in the data. (Figure 8d). Here the uncertainty in the annual estimates is low (CV = 10%) because there were many weeks with efficiency data, the precision of weekly estimates of capture probability was always high owing to large number of recaptures, and because weeks with high catch had reliable estimates of capture probability. The model reliably reproduced the Peterson estimates of capture probability and abundance in this situation.

Estimates for lower Clear Creek for run year 2003 provides and example of a low information case with no efficiency trial data (Figure 8e). Note the very large uncertainty in weekly abundance estimates driven by the high uncertainty in capture probability. For example, on the week beginning January 15 the 95% credible interval for the abundance estimate ranged from approximately 10,000 to 6,000,000 fish. The upper limit was so high because the prior on maximum abundance was based on expanding the catch by an assumed minimum capture probability of 0.005. While uncertainty in weekly abundance estimates was high, the uncertainty for the annual estimate was reasonable (CV = 28%). This occurred because the variance of a summed value (e.g., sum of abundance across all weeks in the run year) is the sum of its individual variances. Relative variation (in CV) is the ratio of the standard deviation and the mean. As the standard deviation is the square root of the variance, relative variation in the annual estimate declines with increases in the number of weeks contributing to the annual estimate (not relatively high catches for many of the 31 weeks in the run year. Results from lower Clear Creek for run year 2020 provide an example of model predictions with a set of continuous weeks without catch data (Figure 8f). The spline component of BT-SPAS-X interpolates abundance for these missing weeks. Given the declining trend in abundance predictions over the last five weeks that were sampled, the model logically interpolates a declining trend for the remaining weeks with no catch data.

Predictions for all sites and run years with sufficient data to run the model are provided in Appendix A. Across all sites and years that were modeled, the mean precision of annual estimates was reasonably high (CV = 0.26, Table 4). The precision of annual estimates depended on a number of factors including the mean capture probability for the site, the number of trap efficiency trials within a year, the number of weeks with both efficiency data and high catch, and the distribution of catches across the run year. For example, catch at Butte Creek was often concentrated in a limited number of weeks (refer to Appendix A). As a result, the precision of the annual estimate of abundance depended more heavily on the lower weekly precision of abundance estimates from a more limited number of weeks. In addition, while capture probability at Butte Creek was high, potentially leading to more precise abundance estimates, the sample size of trap efficiency trials was low (Table 3). This led to greater uncertainty in capture probability and hence greater uncertainty in abundance estimates.

Annual time series of abundance estimates for Chinook outmigrants (all run types combined) are provided in Figure 9. Annual time series of spring-run juvenile outmigrant abundance from Sacramento River tributaries will be a fundamental component of the spring-run JPE model that is being developed. An example of predictions of spring-run proportions by week from the PLAD model for lower Clear Creek in 2018 is provided (Figure 10, refer to Appendix B for full set). Predictions of spring-run proportions at lower Clear Creek in 2018 show a decline in the proportion over the month of January, with moderate precision in weekly estimates (middle panel). The relative error in the annual estimate of spring-run outmigrants (CV = 27%, bottom panel) was higher than the relative error in the estimate for the abundance of all run types (CV = 18%) owing to the uncertainty in weekly spring-run proportions. Predictions of weekly outmigrant abundance and spring-run proportions for all sites and run years with sufficient data are provided in Appendix B. Annual time series for spring-run Chinook outmigrants are provided in Figure 11. Estimates of spring-run proportions at lower Clear Creek were likely too high. This probable bias resulted in a multi-year average juvenile outmigrant abundance at lower Clear Creek that was 15-fold higher than the average from upper Clear Creek (Figure 12). Although some spring-run may spawn downstream of the upper Clear Creek RST site, it is highly improbably that this would explain the large difference in abundance estimates. More likely, the PLAD model is incorrectly assigning some fall-run fish to the spring run.

6 Conclusions

6.1 Future Work, Review, and Guidance on Monitoring

Initial testing and evaluation of BT-SPAS-X indicates it is a suitable tool for translating available RST data from Sacramento River tributaries into weekly and annual estimates of juvenile Chinook salmon outmigrant abundance. Annual estimates of spring-run juvenile outmigrant abundance are an essential component for the spring-run Chinook JPE model.

We anticipate a number of activities to advance the tributary-based outmigration abundance model and its application:

1. The JPE data management team and stream teams will continue to develop the RST database. This work includes adding data that are already collected, adding future data as they becomes available, and filling in missing data in previous versions of the dataset to the extent possible.

   Exploration of the effects of priors (lgN_max) on predicted weekly and annual abundance estimates.
2. The method to include a flow effect on spline-based weekly abundance estimates (Equation 13) has not been implemented yet. We expect there may be limited information with a run year to estimate the effect, perhaps requiring joint estimation of all run years from the same site. This modification would be a substantial undertaking.
3. Predictions of spring-run abundance need to be generated for RST sites that will be used in JPE model development. Additional work on the PLAD model for RST sites on the Feather River is ongoing. Three additional years for Yuba River need to be run through PLAD.

BT-SPAS-X can be used to provide guidance on future sampling to improve the reliability of future RST data. At a qualitative level, recommendations based on results from this chapter include:

1. Conduct mark-recapture efficiency trials in every year at every RST site when possible. Use the historical estimates of capture probability and the precision tools provided here (Figure 2) to determine how many marked fish to release for each efficiency trial to achieve a target precision (e.g. *cv* less than or equal to 0.25). Collection of mark-recapture data in tributaries few trials is particularly important.
2. To the extent possible, ensure efficiency trials are conducted in weeks when catch is anticipated to be elevated. Conducting efficiency trial experiments in weeks with low catch does not lead to significant improvements in the precision of the annual estimate, though it does contribute to the broader capture

probability model. However, given the current large sample size of efficiency trials for May, sites we do not expect parameter values of the capture probability model to change much as more data is added. Closer examination of the predicted variation in weekly abundance estimates over years estimated by BT-SPAS-X can provide guidance on the best time to conduct efficiency trials to maximize precision of annual estimates.

3. Conduct efficiency trials over a wide range of discharges to better inform estimates of the effect of discharge on capture probability. The relationships provided in this chapter can provide guidance on how many marked fish should be released for efficiency trials under more challenging high discharge conditions. For example, capture probability at lower Clear Creek at flows two standard deviations greater than the mean are approximately 0.025 (Figure 5). A horizontal line at 0.025 can be drawn on Figure 2 to determine how many fish must be marked and released to meet a target precision.
4. To the extent possible, sample every stratum within the defined model period (e.g., November through May). BT-SPAS-X can make abundance predictions for missing strata, but assumptions of the maximum possible abundance used to set lgN_max to constrain the upper threshold of abundance estimates introduce bias that is difficult to quantify. Missing strata are particularly problematic when they occur just before or just after periods of high abundance, especially at the beginning or end of the designated run year (e.g., early November, late May). Missing strata will in some cases be unavoidable. Fortunately, the modeling results provided here indicate they are not having significant impacts on the annual abundance estimates in most cases.

Simulation modeling can be used to provide quantitative guidance on future sampling. For example, one could simulate a weekly abundance time series over multiple years, apply different sampling regimes (e.g., 5, 10, 15 efficiency trials/year) to the simulated data, and then examine the effects of the sampling regimes on the bias and precision of annual estimates.

A model predicting juvenile outmigrant abundance based on RST data at the Tisdale and Knights Landing RST sites on the mainstem Sacramento River are described in Chapter 8. Capture probabilities at mainstem sites were much lower and less precise than those from tributaries, so data from tributaries and mainstem sites could not be included in the same model. We have developed a simpler model for the mainstem Sacramento River that independently estimates capture probability and abundance for Tisdale and Knights Landing RST sites. Like the model described here, all efficiency trial data from a site will used to estimate capture probability for each week of a particular run year. However, as only two mainstem sites with similar trapping conditions are available, we could not use a hierarchical structure for site or flow effects as done for the tributary model. Owing to this limitation, and the very low precision of capture probability estimates from mainstem sites seen in the data, annual estimates of abundance for mainstem sites will likely be highly

uncertain compared to those from tributaries. Nevertheless, this result will still prove useful for informing future modeling and monitoring decisions to support the spring-run JPE effort.

6.2 Comparison to the CAMPR Model

In 1997, the Comprehensive Assessment and Monitoring Program (CAMP) was implemented. CAMP was designed to provide a unified protocol for RST data collection and reporting (U.S. Fish and Wildlife Service 2008). The CAMP platform consists of a Microsoft Access database, a desktop user interface to support data entry, and statistical modules for data analysis (i.e., passage estimates). The platform is a template that can be used and maintained locally by each tributary monitoring program for RST data management and analysis. The Comprehensive Assessment and Monitoring Program in R (CAMPR) refers collectively to the CAMP platform and associated R package used to produce passage estimates and reports (Trent and Mitchell 2020). It includes quality assurance reporting, and a series of estimation routines to predict juvenile Chinook outmigration abundance. Here we briefly describe how the estimation routines work so they can be compared to the approaches used in BT-SPAS and BT-SPAS-X.

CAMPR uses information on trapping effort and B-splines to estimate daily catches over a trapping season when the trap was not fishing for periods of greater than two hours and less than seven days. This approach predicts catch each day of a trapping season based on effort (for periods the trap was fished) and spline interpolation (for periods the trap was not fished). Like BT-SPAS and BT-SPAS-X, CAMPR adjusts catches for each stratum (day for CAMPR, weeks for SPAS models) based on effort. This aspect of CAMPR is not problematic. However, CAMPR goes further by interpolating the catch data for periods when the trap was not fished, which in our view is a significant problem. Differences in catch (C) over time are driven by a combination of changes in abundance (N) and changes in trap efficiency (p). Mathematically, this is described by the commonly used equation C=p*N. This equation clarifies that catch can go up or down because N goes up or down if p is constant, or that catch can go up or down with changes in p if N is constant. Returning to the CAMPR approach, by interpolating catch data for periods when the trap is not fished, the model assumes capture probability is the same as adjacent periods when it was not fished. This is not valid in cases when the trap is pulled to high discharge, when trap efficiency will likely be lower compared to adjacent periods when the trap could be fished. BT-SPAS and BT-SPAS-X treat missing catch data more appropriately because they use interpolation to estimate abundance during periods when the trap is not fished, and thus does not need to create data or make assumptions about capture probability during these periods.

CAMPR uses two approaches to estimate trap efficiency. The first only considers efficiency data from a single trapping season, similar to BT-SPAS. However, CAMPR uses a very ad-hoc approach in this situation. If there are less than 10 trials in the

season, an average efficiency value is calculated by the ratio of the sum of recaptures to the sum of releases, and is then applied to all days of the trapping season to estimate daily abundance (it is essentially a pooled Peterson estimate). When there are ten or more trials in a season, CAMPR uses a B-spline fit to daily efficiency estimates to calculated efficiency for each day of the run. The spline parameters are fit based on the same data likelihood (r~dbin(p,R)) used in BT-SPAS and BT-SPAS-X. However, by doing the spline interpolation, CAMPR assumes a lack of independence of efficiency values over time, while BT-SPAS and -X models assume they are independent over time, but can change with covariates. CAMPR also implements the B-spline estimation for capture probability by using a stepwise AIC approach to determine how many knots to use for the spline. In contrast, the approach to fitting the spline method for estimating abundance (not efficiency) in BT-SPAS and BT-SPAS-X models is much more elegant and robust because it adjusts the spline tension (Bayesian penalized spline) based on the amount of information in the model about variation in abundance (not catch) over time. Following standard statistical procedures advised for Bayesian penalized splines, the spline stiffness, rather than the number of knots, is adjusted.

CAMPR also includes an enhanced efficiency model, where multiple years of RST data from a site are combined, and covariates are used to predict trap efficiency. This aspect of the CAMPR approach is similar to BT-SPAS-X (that is, it considers data from multiple years), but the CAMPR approach does not consider the efficiency data in a hierarchal way like BT-SPAS and BT-SPAS-X. For example, if an information-rich efficiency trial results in an efficiency value considerably higher than adjacent estimates, the CAMPR spline approach will use an interpolated value that may be well below the data-driven value. The hierarchical model with random effects used in BT-SPAS and BT-SPAS-X only substantively changes data-driven efficiency estimates if they are weakly supported by the data (because few recaptures were obtained). The hierarchical structure also properly accounts for the greater uncertainty in strata where efficiency trials are not conducted or when efficiency trial data for a given week contains limited information about capture probability.

Methods used in BT-SPAS and BT-SPAS-X have significant advantages over CAMPR. The approach used in BT-SPAS-X largely follows BT-SPAS, a published, fully vetted, and widely applied model developed in part by an internationally-recognized mark-recapture expert (C. Schwarz). We see no point in making a comparison of BT-SPAS-X and CAMPR abundance estimates for sites and years when both are available, because of the methodological problems in CAMPR described above.

7 References

Arnason, AN, CW Kirby, CJ Schwarz, and JR Irvine. 1996. "Computer Analysis of Data from Stratified Mark-Recovery Experiments for Estimation of Salmon Escapements and Other Populations." *Canadian Technical Report of Fisheries and Aquatic Sciences* 2106. https://waves-vagues.dfo-mpo.gc.ca/Library/197629.pdf

Gelman, A, and DB Rubin. 1992. "Inference from Iterative Simulation Using Multiple Sequences." *Statistical Science* 7(4):457–511. https://sites.stat.columbia.edu/gelman/research/published/itsim.pdf

Bonner, SJ, and CJ Schwarz. 2011. "Smoothing Population Size Estimates for Time-Stratified Mark–Recapture Experiments Using Bayesian P-Splines." *Biometrics* 67(4):1498–1507. https://academic.oup.com/biometrics/article/67/4/1498/7381210

Bonner, SJ. 2008. "Heterogeneity in Capture-Recapture: Bayesian Methods to Balance Realism and Model Complexity." Ph.D. Thesis. Simon Fraser University. http://www.stat.sfu.ca/content/dam/sfu/stat/alumnitheses/MiscellaniousTheses/Bonner-2008.pdf

Cordoleani, F, CC Phillis, AM Sturrock, AM FitzGerald, A Makassian, GE Whitman, PK Weber, and RC Johnson. 2021. "Threatened salmon rely on a rare life history strategy in a warming landscape." *Nature Climate Change*. 11:982–988. https://doi.org/10.1038/s41558-021-01186-4

McDonald, T, and J Mitchell. 2020. "CAMPR analysis documentation: Methods embedded in the CAMPR platform for juvenile salmonid passage estimation from rotary screw trap data." Filename CAMPRdoc, last revision June 11, 2020. [Published where; volume and pages or URL. Match style of other references.]

Millar, RB, and MJ Anderson. 2004. "Remedies for pseudoreplication." *Fisheries Research* 70:387–407. https://doi.org/10.1016/j.fishres.2004.08.016

Pilger, TJ, ML Peterson, D Lee, A Fuller, and D Demk. 2019. "Evaluation of Long-Term Mark-Recapture Data for Estimating Abundance of Juvenile Fall-Run Chinook Salmon on the Stanislaus River from 1996 to 2017." *San Francisco Estuary and Watershed Science* 17(1). https://doi.org/10.15447/sfews.2019v17iss1art4

R Core Team. 2024. *R: A Language and Environment for Statistical Computing: Reference Index.* Version 4.4.1 R Foundation for Statistical Computing, Vienna, Austria. https://cran.r-project.org/doc/manuals/r-release/fullrefman.pdf.

Schwarz, CJ, D Pickard, K Marine and SJ Bonner. 2009. *Trinity River Restoration Program Juvenile Salmonid Outmigrant Monitoring Evaluation, Phase II*. Final Technical Memorandum. USBR Task Order 06A0204097G. Prepared for Trinity River Restoration Program. Prepared by ESSA Technologies, Ltd., Simon Fraser University Department of Statisitics, and North State Resources, Inc. December. https://www.trrp.net/DataPort/doc.php?id=369

Som, Nicholas A, and William D Pinnix. 2014. *Evaluation of Reductions in Sampling and Mark-Recapture Effort on the Bias and Precision of Juvenile Chinook Salmon Outmigrant Estimates on the Trinity River, California*. Arcata Fisheries Technical Report TR 2014-20. Prepared for the U.S. Fish and Wildlife Service. https://www.researchgate.net/publication/280923594_Evaluation_of_Reductions_in_Sampling_and_Mark-Recapture_Effort_on_the_Bias_and_Precision_of_Juvenile_Chinook_Salmon_Outmigrant_Estimates_on_the_Trinity_River_California

Spiegelhalter, DJ, A Thomas, NG Best, and D Lunn. 2003. *WinBUGS User Manual*. Version 1.4. MRC Biostatistics Unit, Institute of Public Health, Cambridge, UK. https://legacy.voteview.com/pdf/WINBUGSmanual_2.pdf

Stan Development Team. 2024. *Stan Users Guide*. Version 2.35. https://mc-stan.org.

Sturtz, S, U Legges, and A Gelman. 2005. "R2WinBGS: A Package for Running WinBUGS from R." *Journal of Statistical Software* 3:1–16. https://www.jstatsoft.org/article/view/v012i03

Tables and Figures

Tables

Table 1. Weeks of Sampling by Run Year and Rotary Screw Trap Site

Number of weeks of sampling by run year and rotary screw trap (RST) site between November 4 and May 27. Run year 't' includes weeks from November 4 through December in calendar year 't-1' and January through May 27 in calendar year 't'. Refer to Figure 1 for locations of RST sites.

Run Year	Battle Creek	Lower Battle Creek	Butte Creek	Upper Clear Creek	Lower Clear Creek	Deer Creek	Mill Creek	Yuba River	Eye Riffle	Live Oak	Herringer Riffle	Steep Riffle	Sunset Pumps	Gateway Riffle	Lower Feather
1996	-	-	31	-	-	31	31	-	-	-	-	-	-	-	-
1997	-	-	-	-	-	-	-	-	-	-	-	-	-	-	-
1998	-	-	-	-	-	-	-	-	31	31	-	-	-	-	-
1999	31	31	31	-	31	-	-	-	31	31	-	-	-	-	-
2000	31	31	31	-	31	31	31	-	31	31	-	-	-	-	-
2001	-	-	31	-	31	31	31	31	31	31	-	-	-	-	-
2002	31	31	31	-	31	31	31	31	31	-	20	-	-	-	-
2003	-	31	31	-	31	31	31	-	31	-	31	-	-	-	-
2004	31	31	31	31	31	-	-	31	31	-	31	-	-	-	-
2005	31	31	-	31	31	31	31	31	31	-	31	-	-	-	-
2006	31	-	-	31	31	-	31	31	31	-	31	-	-	-	-
2007	-	-	31	31	31	31	31	31	-	-	-	31	-	-	-
2008	31	-	31	31	31	-	31	31	-	-	31	31	-	-	-
2009	31	-	-	-	31	31	-	31	-	-	-	31	-	-	-
2010	31	-	-	31	31	31	31	-	-	-	-	31	31	-	-
2011	31	-	-	31	31	-	-	-	-	-	-	31	31	-	-
2012	31	-	-	31	31	-	-	-	-	-	31	31	-	-	-
2013	31	-	31	31	31	-	-	-	-	-	31	-	-	31	-
2014	31	-	31	31	31	-	-	-	-	-	31	-	-	31	-
2015	-	-	31	31	31	-	-	-	-	-	31	-	-	-	-
2016	31	-	31	31	31	-	-	-	-	-	-	-	-	-	-
2017	31	-	-	31	31	-	-	-	-	-	-	-	-	-	-
2018	31	-	31	31	31	-	-	-	31	-	31	-	-	-	-
2019	31	-	-	31	31	-	-	-	31	-	31	-	-	-	-
2020	31	-	31	31	31	-	-	-	31	-	31	-	-	-	-
2021	31	-	31	31	31	-	-	-	-	-	-	-	-	-	-
2022	31	-	31	31	31	-	31	-	31	-	31	-	-	-	22
2023	31	-	31	-	31	31	31	31	31	-	31	-	-	-	-
2024	31	-	31	-	31	31	31	31	31	-	31	-	-	-	-
Total Years	22	6	19	18	26	11	13	10	15	4	16	6	2	2	1

Table 2. Efficiency Trials by Run Year and Rotary Screw Trap Site

Number of efficiency trials by run year and RST site. Run Year r ‘t’ includes weeks from October through December in calendar year ‘t-1’ and January through June in calendar year ‘t.’

Run Year	Battle Creek	Lower Battle Creek	Butte Creek	Upper Clear Creek	Lower Clear Creek	Deer Creek	Mill Creek	Yuba River	Eye Riffle	Live Oak	Herringer Riffle	Steep Riffle	Sunset Pumps	Gateway Riffle	Lower Feather
1996	-	-	-	-	-	-	-	-	-	-	-	-	-	-	-
1997	-	-	-	-	-	-	-	-	-	-	-	-	-	-	-
1998	-	-	-	-	-	-	-	-	-	-	-	-	-	-	-
1999	-	-	-	-	-	-	-	-	3	2	-	-	-	-	-
2000	-	-	-	-	-	-	-	-	8	6	-	-	-	-	-
2001	-	-	-	-	-	-	-	-	8	9	-	-	-	-	-
2002	-	-	-	-	-	-	-	-	9	-	7		-	-	-
2003	-	-	-	-	-	-	-	-	10	-	9		-	-	-
2004	12	-	-	15	12	-	-	-	14	-	15		-	-	-
2005	19	-	-	19	19	-	-	-	15	-	18		-	-	-
2006	5	-	-	15	14	-	-	-	11	-	6		-	-	-
2007	-	-	-	18	17	-	-	-	-	-	-	16	-	-	-
2008	16	-	-	16	16	-	-	-	-	-	11	20	-	-	-
2009	14	-	-	-	19	-	-	-	-	-	-	13	-	-	-
2010	7	-	-	4	7	-	-	-	-	-	-	19	12	-	-
2011	8	-	-	4	13	-	-	-	-	-	-	14	9	-	-
2012	10	-	-	6	14	-	-	-	-	-	18	15	-	-	-
2013	6	-	-	2	14	-	-	-	-	-	18	-	-	16	-
2014	2	-	-	6	6	-	-	-	-	-	11	-	-	11	-
2015	-	-	-	4	4	-	-	-	-	-	12	-	-	-	-
2016	3	-	-	12	14	-	-	-	-	-	-	-	-	-	-
2017	4	-	-	4	6	-	-	-	-	-	-	-	-	-	-
2018	5	-	-	3	7	-	-	-	13	-	13	-	-	-	-
2019	3	-	-	1	4	-	-	-	10	-	8	-	-	-	-
2020	3	-	-	3	8	-	-	-	17	-	18	-	-	-	-
2021	7	-	7	6	4	-	-	-		-	-	-	-	-	-
2022	-	-	3	-	-	-	3	-	12	-	9	-	-	-	6
2023	4	-	7	-	2	6	6	16	9	-	7	-	-	-	-
2024	3	-	2	-	4	3	4	18	11	-	10	-	-	-	-
Total	131	0	19	138	204	9	13	34	150	17	190	97	21	27	6

Table 3. Trap Efficiency by Rotary Screw Trap Site

Statistics on capture probability (trap efficiency) by RST site. The last column shows the percentage of the total number of trials (mark-recapture experiments) where the coefficient of variation (CV) of capture probability was less than or equal to 0.25 (i.e., relatively precise estimates).

Site	Efficiency Trials	Mean Efficiency	Proportion of Trials with CV< 0.25
Battle Creek	131	0.05	0.76
Butte Creek	19	0.27	0.84
upper Clear Creek	138	0.09	0.86
lower Clear Creek	204	0.05	0.65
Deer Creek	9	0.02	0.00
Mill Creek	13	0.06	0.54
Yuba River	34	0.01	0.21
Eye Riffle	150	0.03	0.69
Live Oak	17	0.02	0.29
Herringer Riffle	190	0.02	0.58
Steep Riffle	97	0.16	0.94
Sunset Pumps	21	0.02	0.57
Gateway Riffle	27	0.02	0.67
Lower Feather	6	0.01	0.33

Table 4. Coefficient of Variation in Annual Estimates of Juvenile Outmigrant Abundance of Chinook Salmon

Statistics for the CV in annual estimates of juvenile outmigrant abundance of Chinook salmon (all run types) by RST site. Statistics are the minimum CV across years, the mean across years, and the maximum across years. PLAD predictions were not currently available for three years at the Hallwood site, but will be available soon.

Run Type	Site	Years of Data	CV Minimum	CV Mean	CV Maximum
All	Battle Creek	22	0.10	0.31	0.49
All	upper Clear Creek	18	0.11	0.33	0.78
All	lower Clear Creek	26	0.08	0.22	0.41
All	Deer Creek	12	0.16	0.21	0.32
All	Mill Creek	13	0.18	0.28	0.43
All	Butte Creek	19	0.17	0.41	0.80
All	Yuba River	10	0.03	0.09	0.19
Spring Run	Battle Creek	22	0.11	0.32	0.49
Spring Run	upper Clear Creek	18	0.11	0.33	0.78
Spring Run	lower Clear Creek	26	0.23	0.31	0.63
Spring Run	Deer Creek	12	0.18	0.24	0.33
Spring Run	Mill Creek	13	0.25	0.35	0.50
Spring Run	Butte Creek	19	0.17	0.41	0.80
Spring Run	Yuba River	7	0.14	0.17	0.21

Figures

Figure 1. Map of Rotary Screw Trap Sites

Map of the Sacramento River and tributaries showing the location of RST sites considered for use in the spring-run juvenile production estimate (JPE) modeling. Note: all references to the Butte Creek RST in this document are for the Parrot-Phelan Dam site.

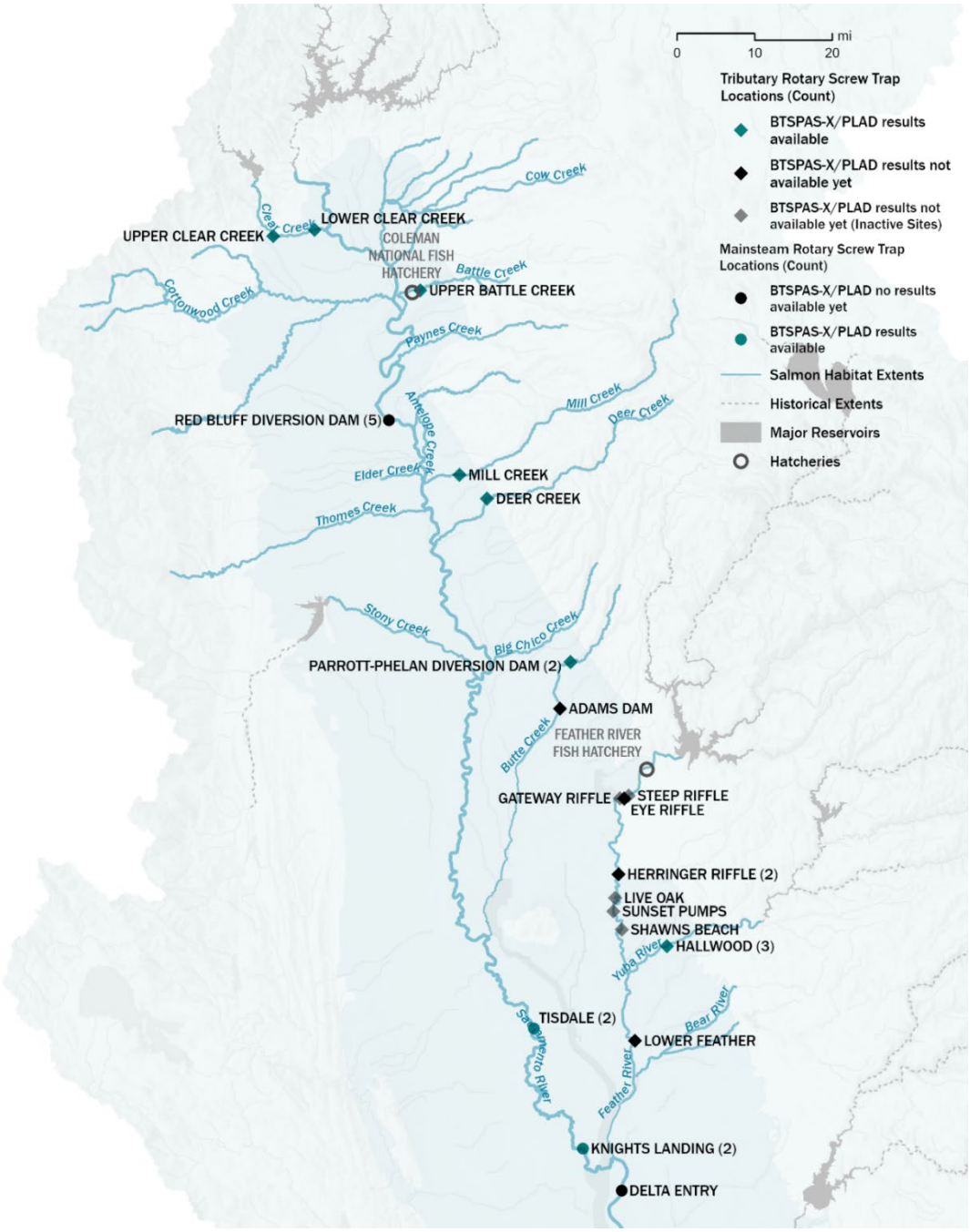

Figure 2. Capture Probability For Juvenile Chinook Salmon

Capture probability (trap efficiency) for juvenile Chinook salmon from Central Valley RST sites. Red lines are contours showing how the precision of capture probability estimates varies as a function of the number of marks released and the capture probability. Contour values represent the CV of capture probability estimates. The numbers in the title of each plot show total number of mark-recapture experiments conducted. The horizontal black line is the simple average of all capture probability values.

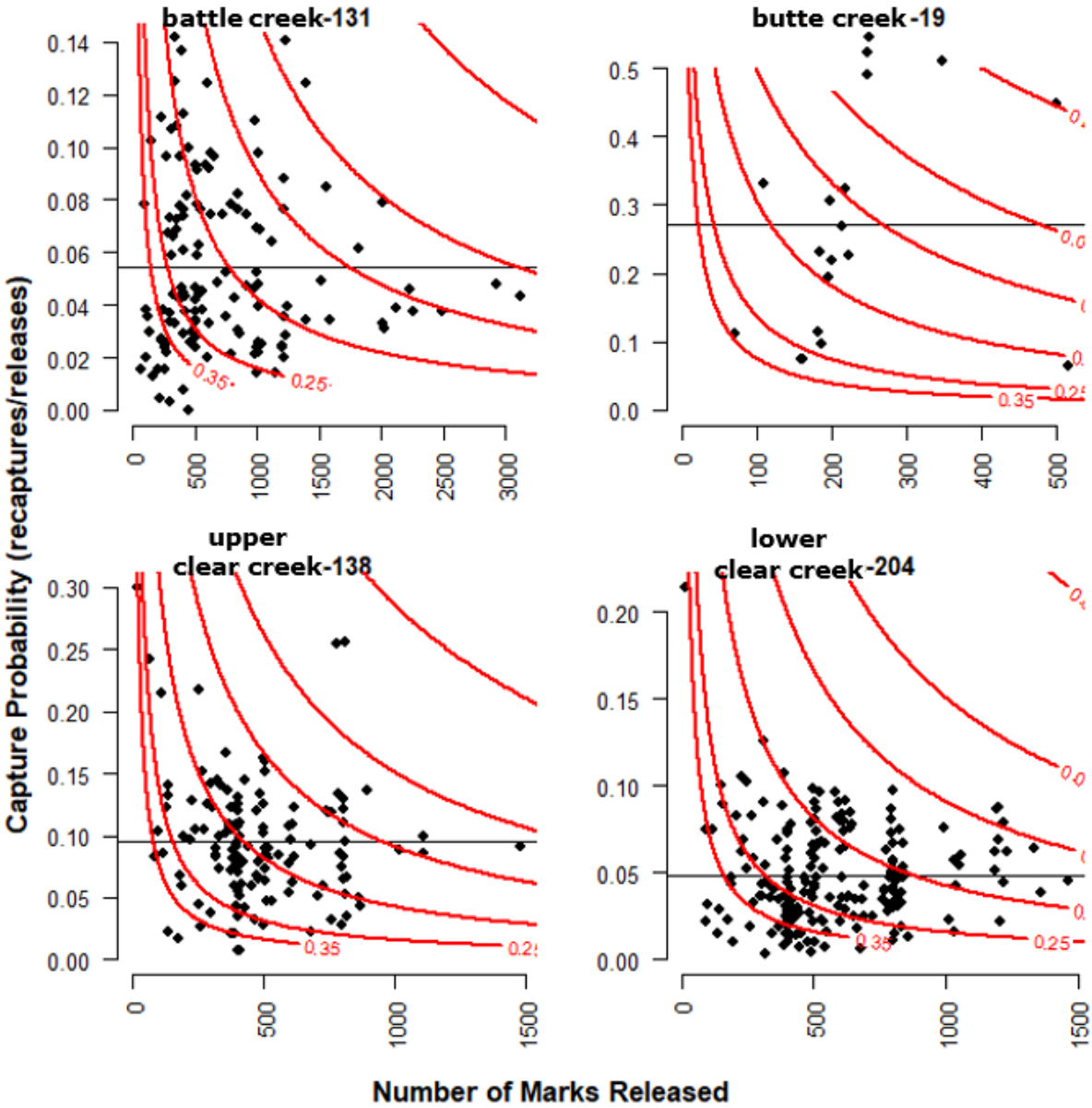

Figure 2. Continued

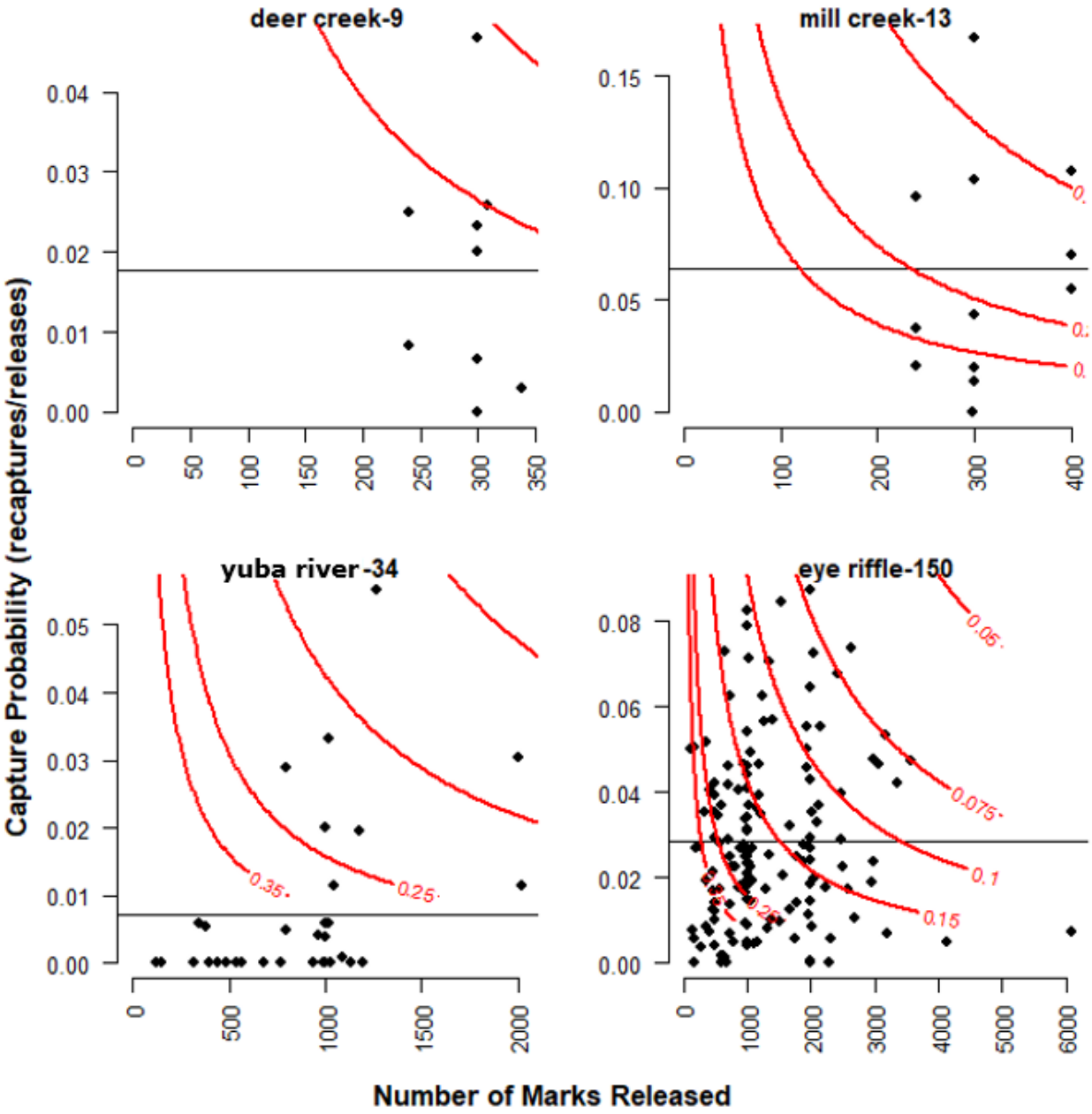

Figure 2. Continued

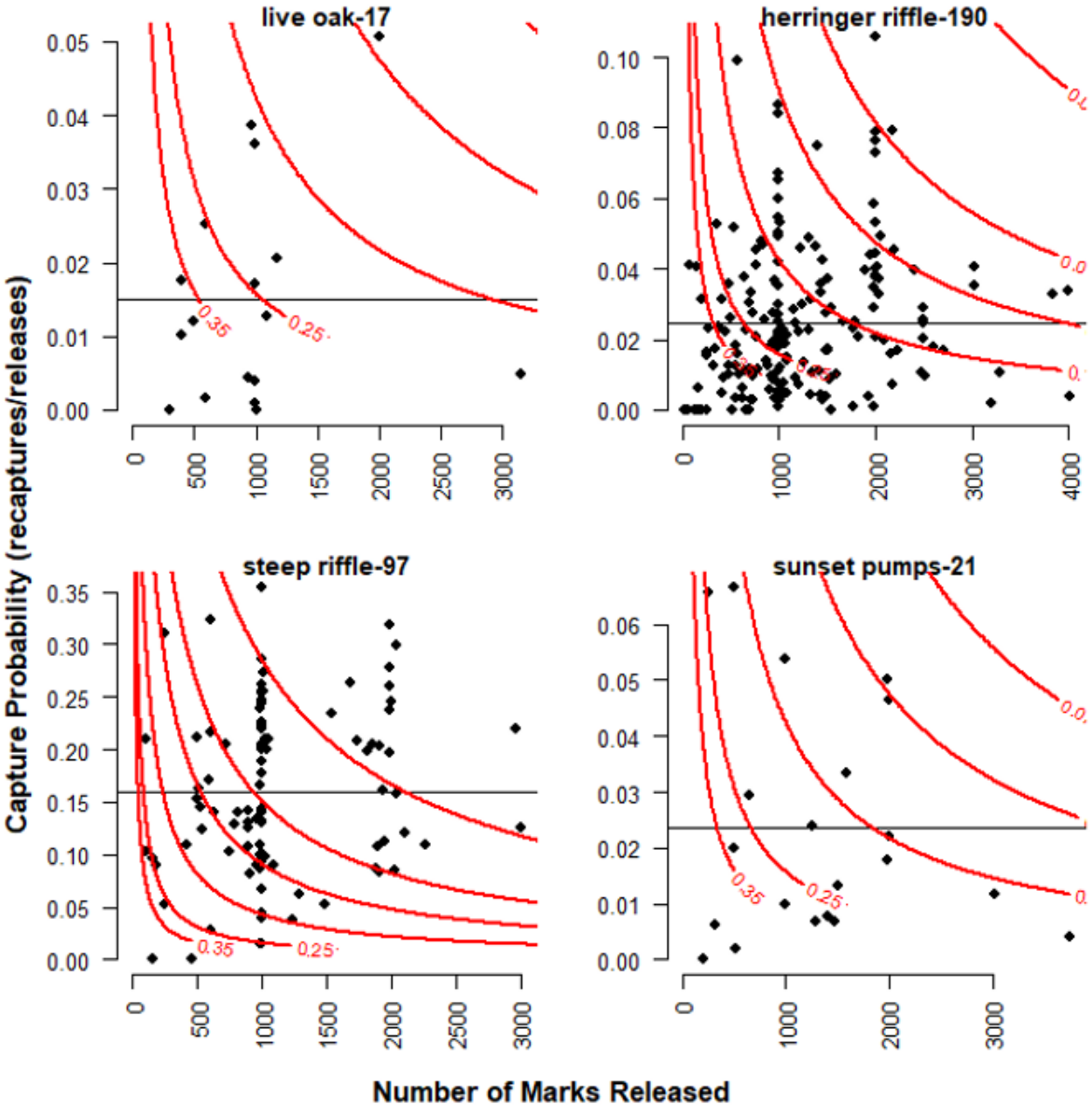

Figure 2. Continued

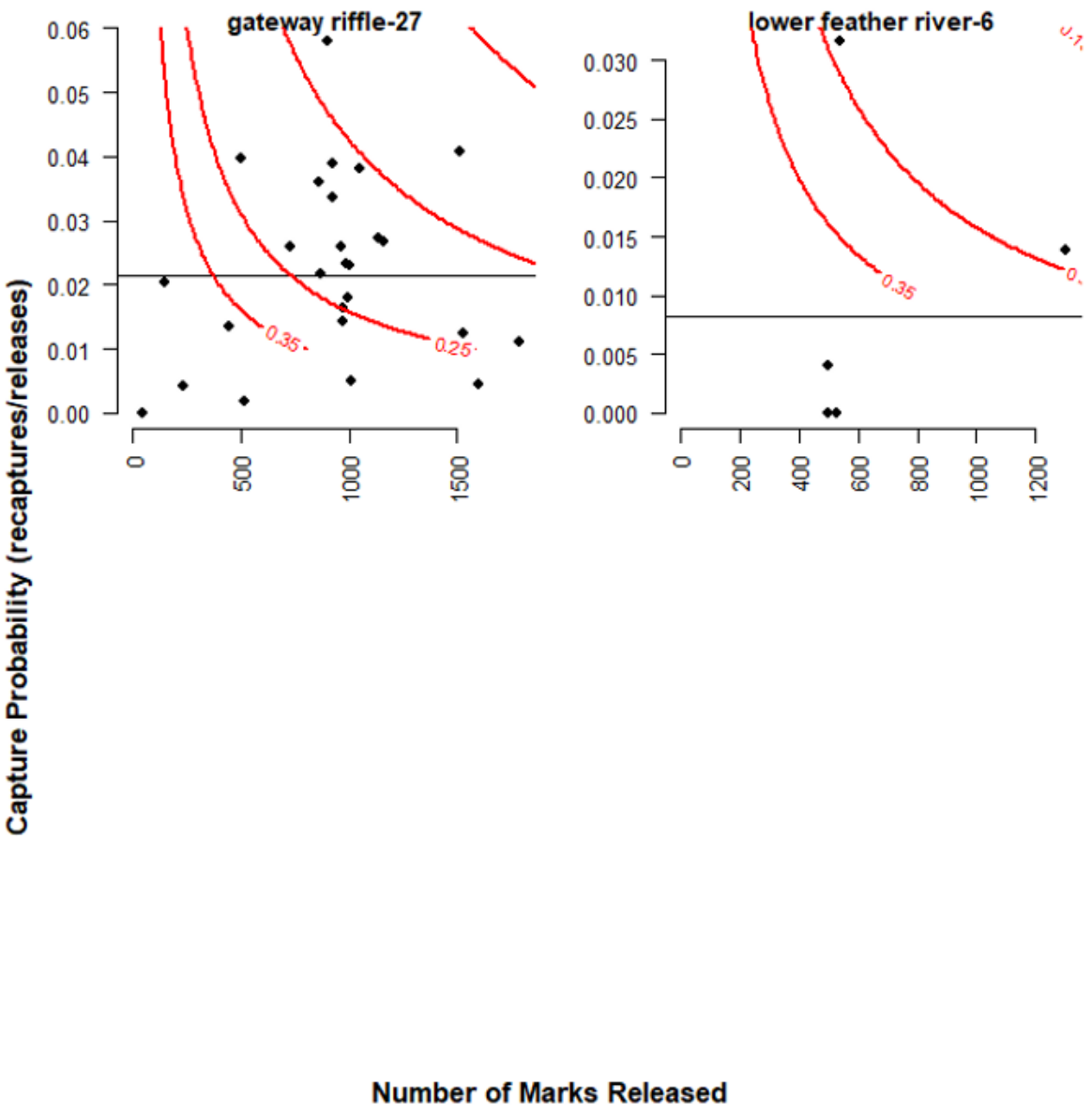

Figure 3. Directed Acyclic Graph Describing Relationship Among Estimated Parameters

Directed acyclic graph (DAG) describing the relationship among estimated parameters (stochastic nodes denoted by Greek letters within ovals) and data (Roman bolded letters in squares). Vertical position in the DAG denotes the parent-child relationship among nodes. The red triangle denotes that capture probability estimates influence abundance estimates but the converse does not occur. For simplicity, subscripts for site, year, and week are not shown.

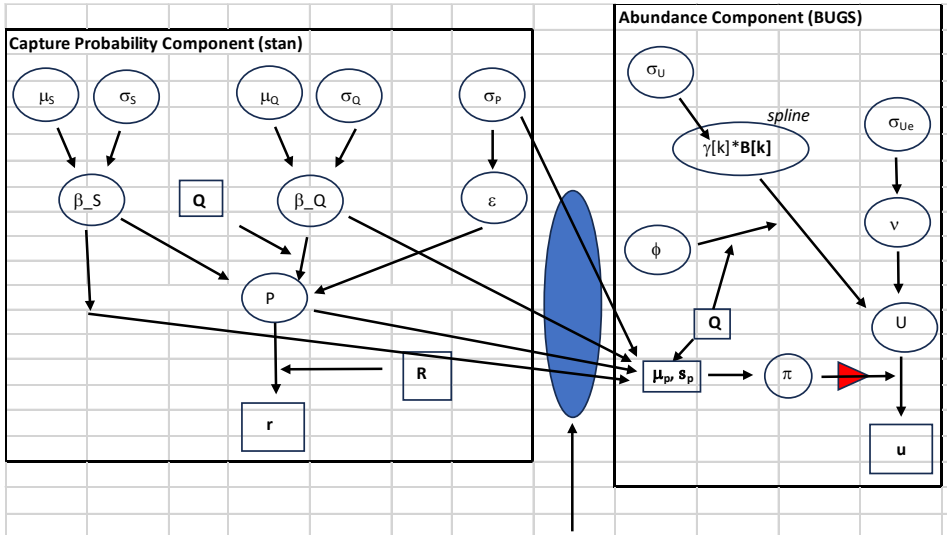

Capture Probability Model	
μ_S	mean of hyper-distribution for site effect
σ_S	standard deviation of hyper-distribution for site effect
μ_Q	mean of hyper-distribution for flow effect
σ_Q	standard deviation of hyper-distribution for flow effect
σ_p	standard deviation of zero-centered normal distribution for unexplained error
β_S	site effect on capture probability for each site
β_Q	flow effect on capture probability for each site
P	Capture probability (trap efficiency)
ε	unexplained error in capture probability
r	observed recaptures
R	observed releases
Q	observed weekly average flow

Abundance Model	
σ_U	standard deviation controlling flexibilti of spline weekly abundance curve
γ	spline coefficient for each spline knot k with basis function **B**
ϕ	parameter controlling effect of flow on predicted weekly abundance
σ_{Ue}	standard deviation controlling extent of non-spline variation in weekly abundance
ν	weekly deviate added to spline-predicted weekly abundance
U	predicted weekly abundance
u	observed weekly catch
Q	observed weekly average flow
B	Basis function of each spline node
μ_p	mean of weekly capture probability
σ_p	standard deviation of weekly capture probabilty
π	weekly capture probability

square boxes and bolded variables are data or variables treated as data
ovals denote stochastic nodes (things that are estimated)
vertical position denotes parent-child relationships. E.g., the site-specific intercept beta_S is a child of the site-effect hyper distribution defined by mu_S and sd_S
for simplicity of diagram, subscripts for site, year, and week are not shown
red triangle denotes use of cut() function so abundance model cannot influence weekly means and standard deviations of capture probability
cut() function removed from stan version of model

Figure 4. Mean and Intervals from Average Capture Probabilities

The mean and 95% credible intervals from the posterior estimates of RST site-specific average capture probabilities (β_S_s of Equation 11, black points and horizontal error bars). The black curved line shows the mean estimate of the hyper-distribution for β_S_s (Equation 12a). Open blue points are the average of the ratios of recaptures to releases.

Figure 4a. All sites contribute to hyper-distribution parameters and use the hyper-distribution for site-specific priors

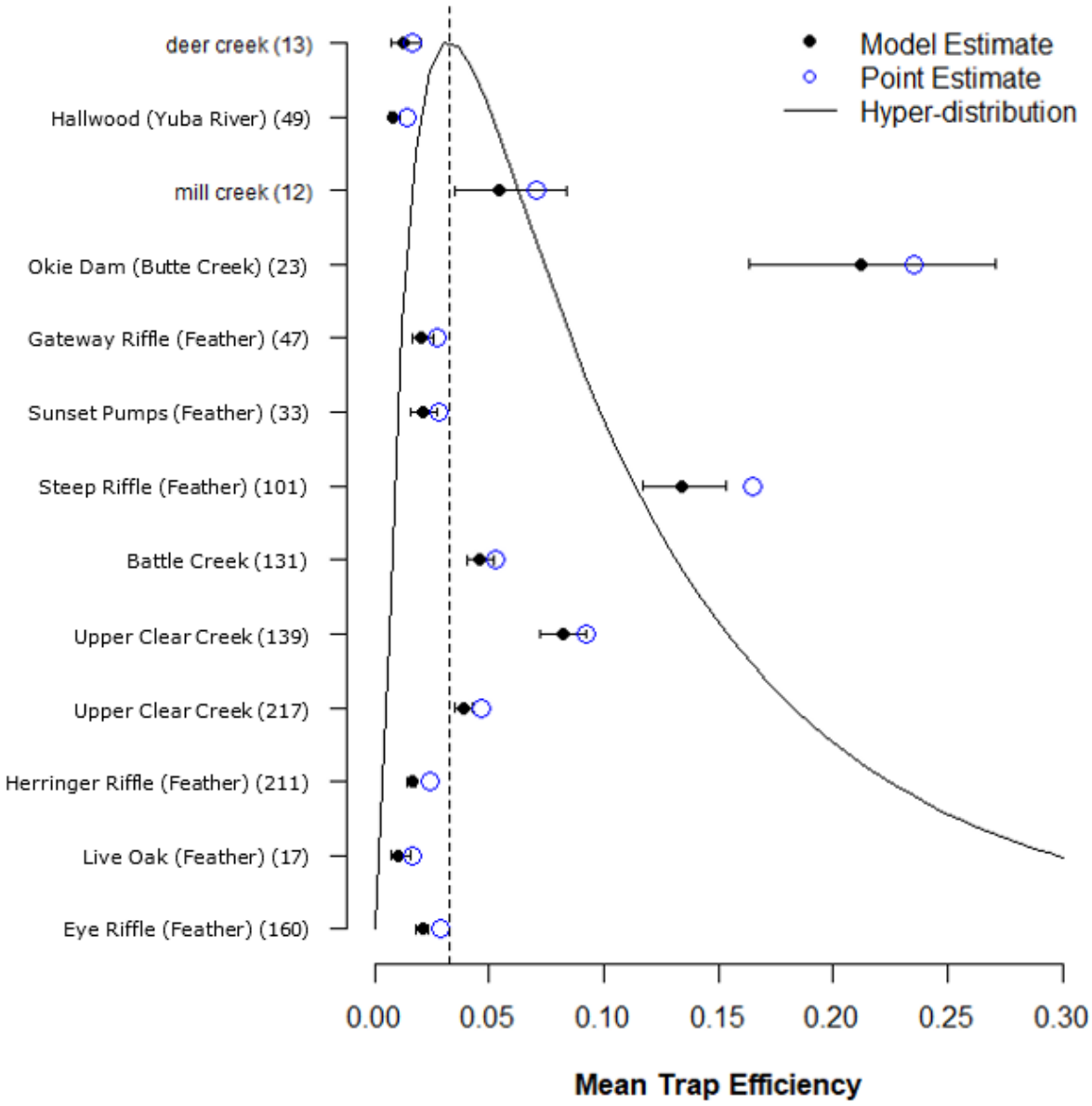

Figure 4b. Butte Creek and Steep Riffle sites excluded from estimation of hyper-distribution parameters and uninformative uniform site-specific priors are used for these sites

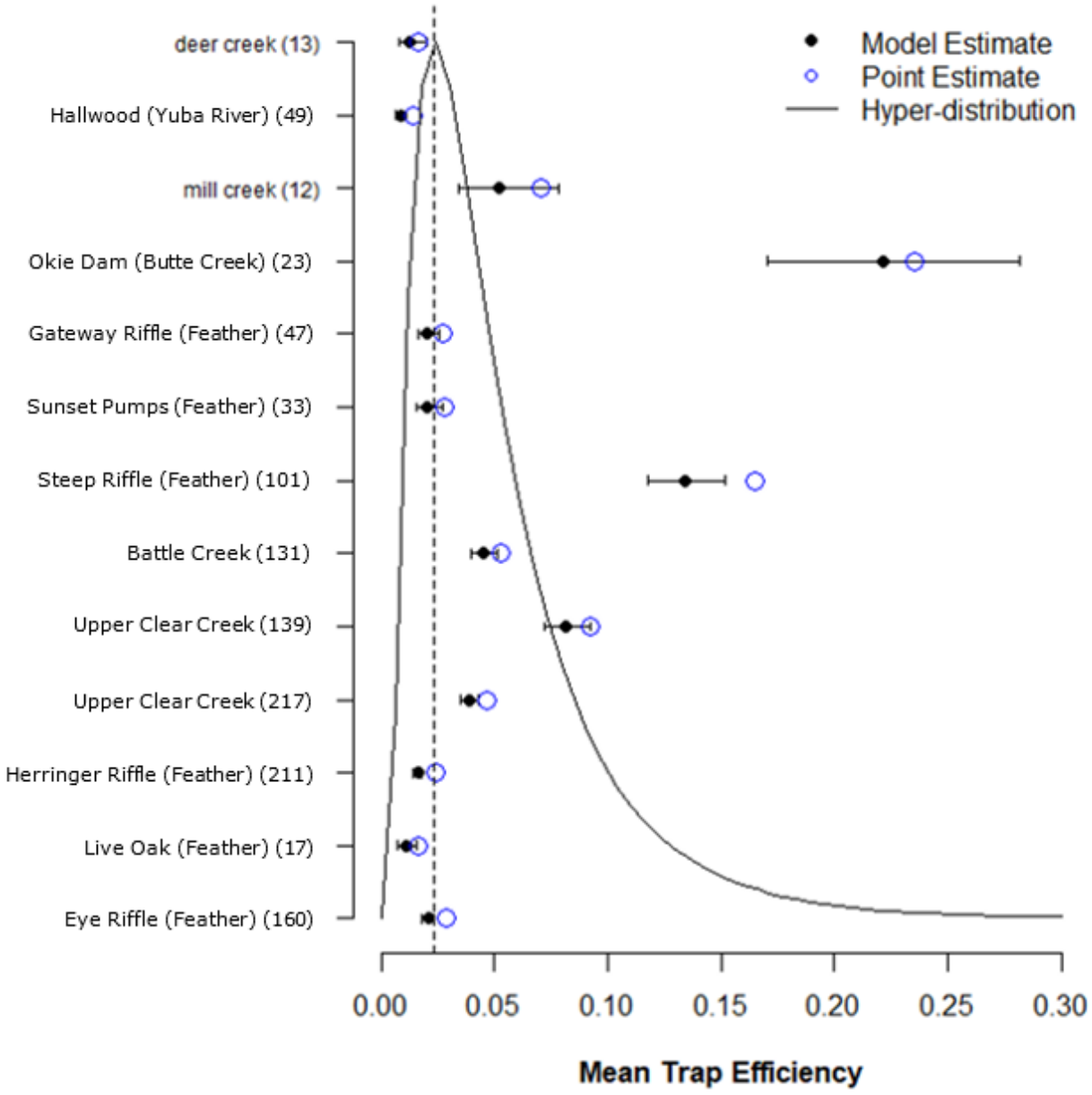

Figure 5. Means 95% Credible Intervals Between Standardized Discharge and Capture Probability

Means (lines) and 95% credible intervals (shaded areas) of RST site-specific relationships between standardized discharge and capture probability. Points are the trial-specific capture probabilities computed based on the ratio of recaptures to releases. Note the y-axis value at the intersection of the vertical lines (mean discharge) and the predicted capture probability line represents the means of the transformed β_S estimates shown in Figure 4.

Figure 5a. All sites contribute to hyper-distribution parameters and use the hyper-distribution for site-specific priors

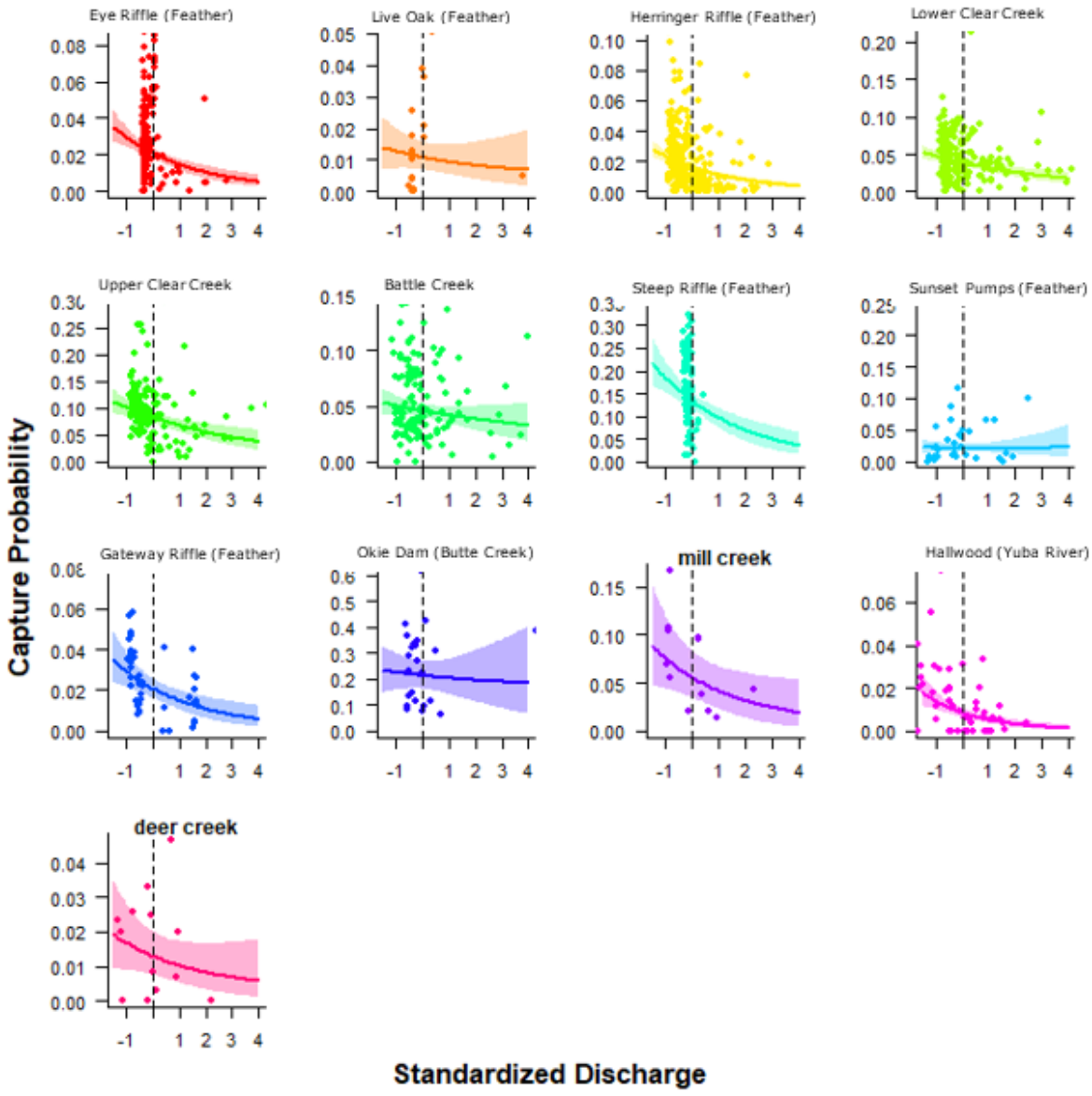

Figure 5b. Butte Creek and Steep Riffle sites excluded from estimation of hyper-distribution and uninformative uniform site-specific priors are used for these sites

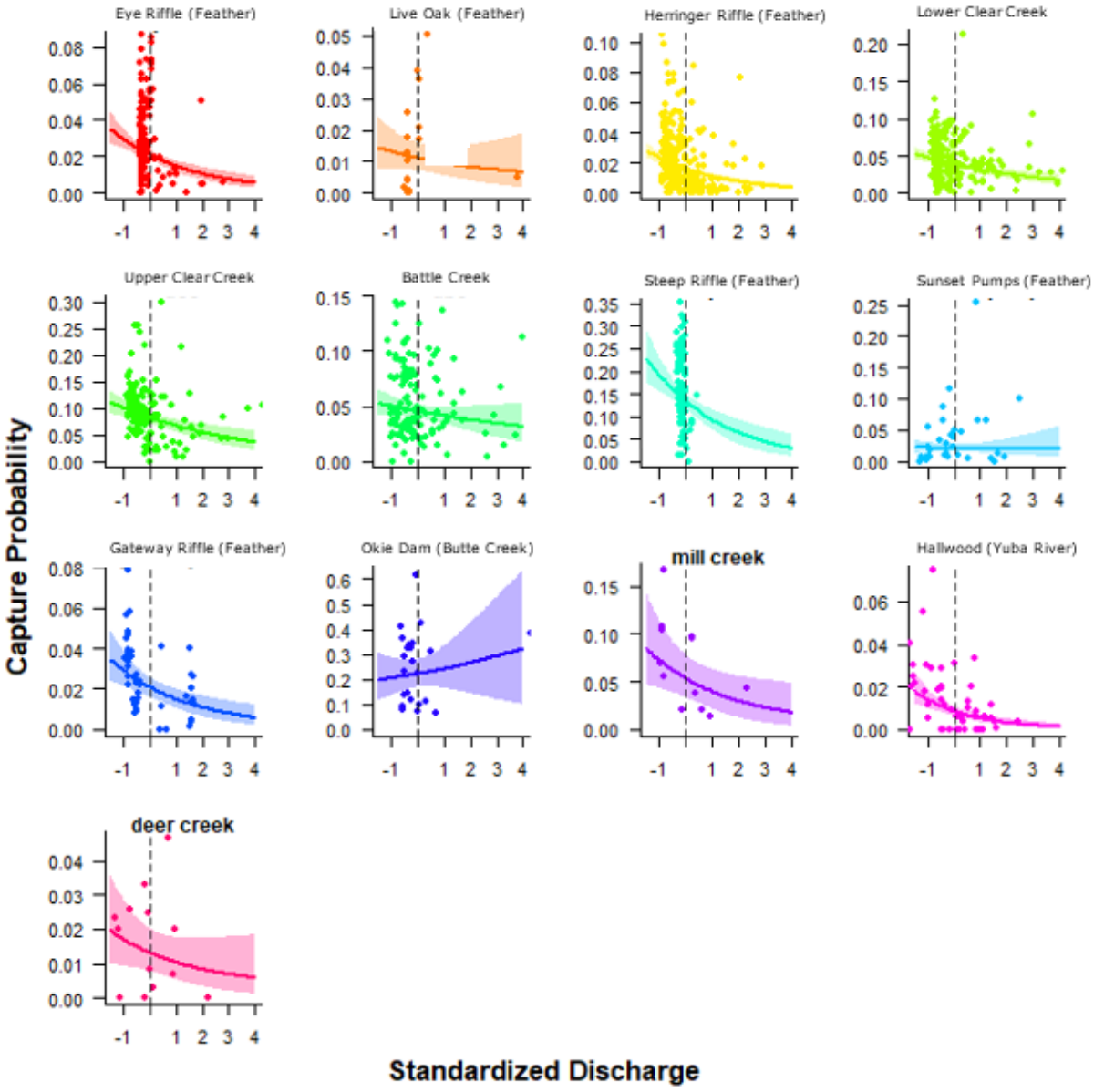

Figure 6. Relationship Between Average Fork Length and Capture Probability

The relationship between the average fork length for marked fish that were released and capture probability.

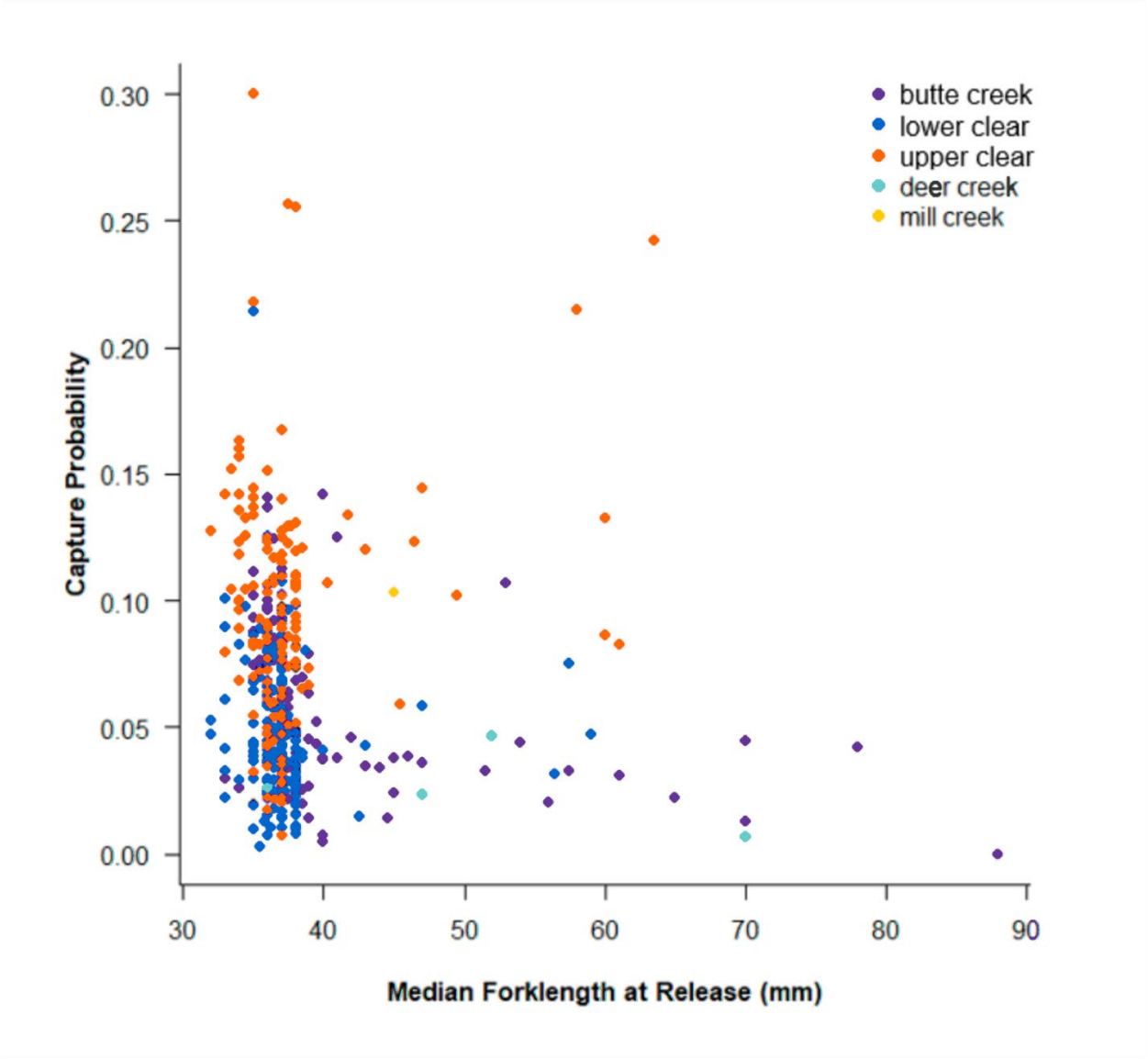

Figure 7. Effect of Discharge and Capture Probability

Effect of discharge and the origin of marked fish that are released on capture probability in Battle Creek. Lines and shaded areas show the mean estimates and 95% credible intervals, respectively.

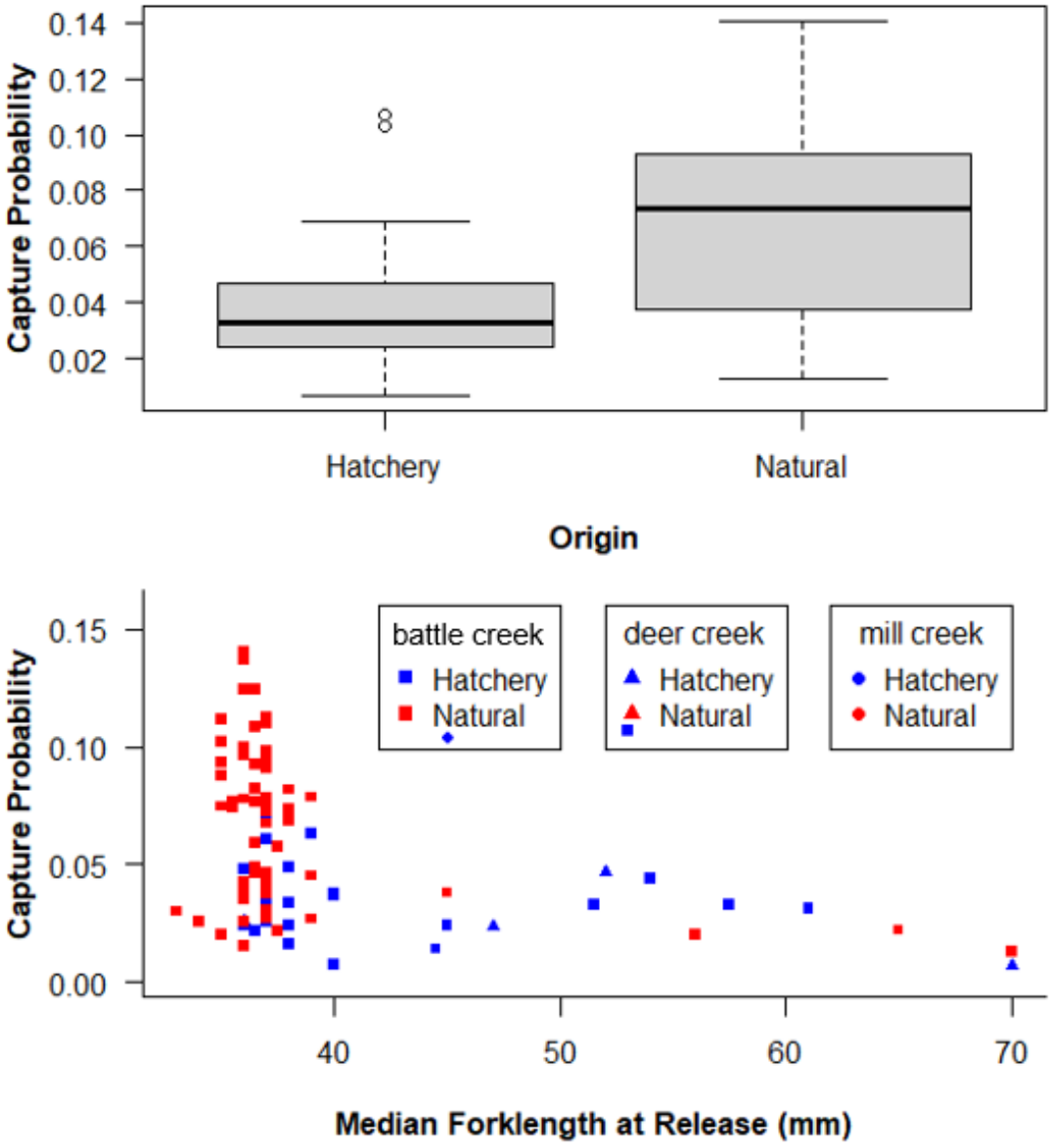

Figure 8. Predicted Abundance of Juvenile Outmigrant Chinook Salmon and Capture Probability By Weekly Strata

Predicted abundance of juvenile outmigrant Chinook salmon (all run types and fry and smolt life stages combined, top panel) and capture probability (bottom panel) by weekly strata for select RSTs sites and run years. The height of the bars and black error bars show the medians and 95% credible intervals predicted by BT-SPAS-X. Bars in the top panels with dots above them and no open circles or numbers above them identify strata with no sampling data; bars in the bottom panel identify strata with no mark-recapture data. Numbers at the top of each plot show the unmarked catch (u, top panel), and the number of recaptures (r) and releases (R, bottom panel). Open circles show the Peterson estimates of abundance (U=u/p, error bars show 95% confidence intervals)) and capture probability (p=r/R). The line with points shows the average weekly discharge. The title shows the median total abundance estimate for the run year with 95% credible intervals in parentheses. The CV of the annual abundance estimate is also shown.

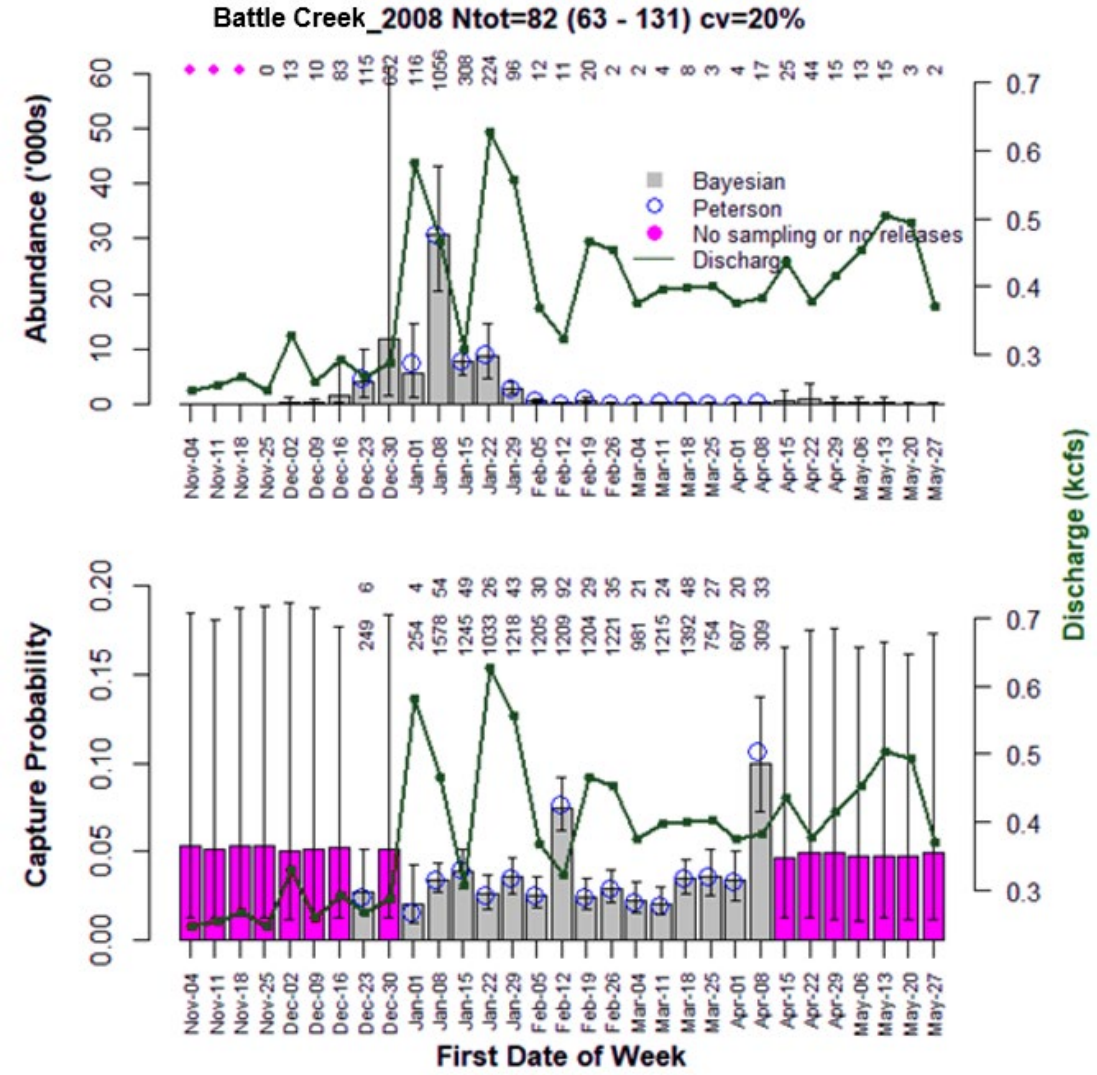

Figure 8, Continued

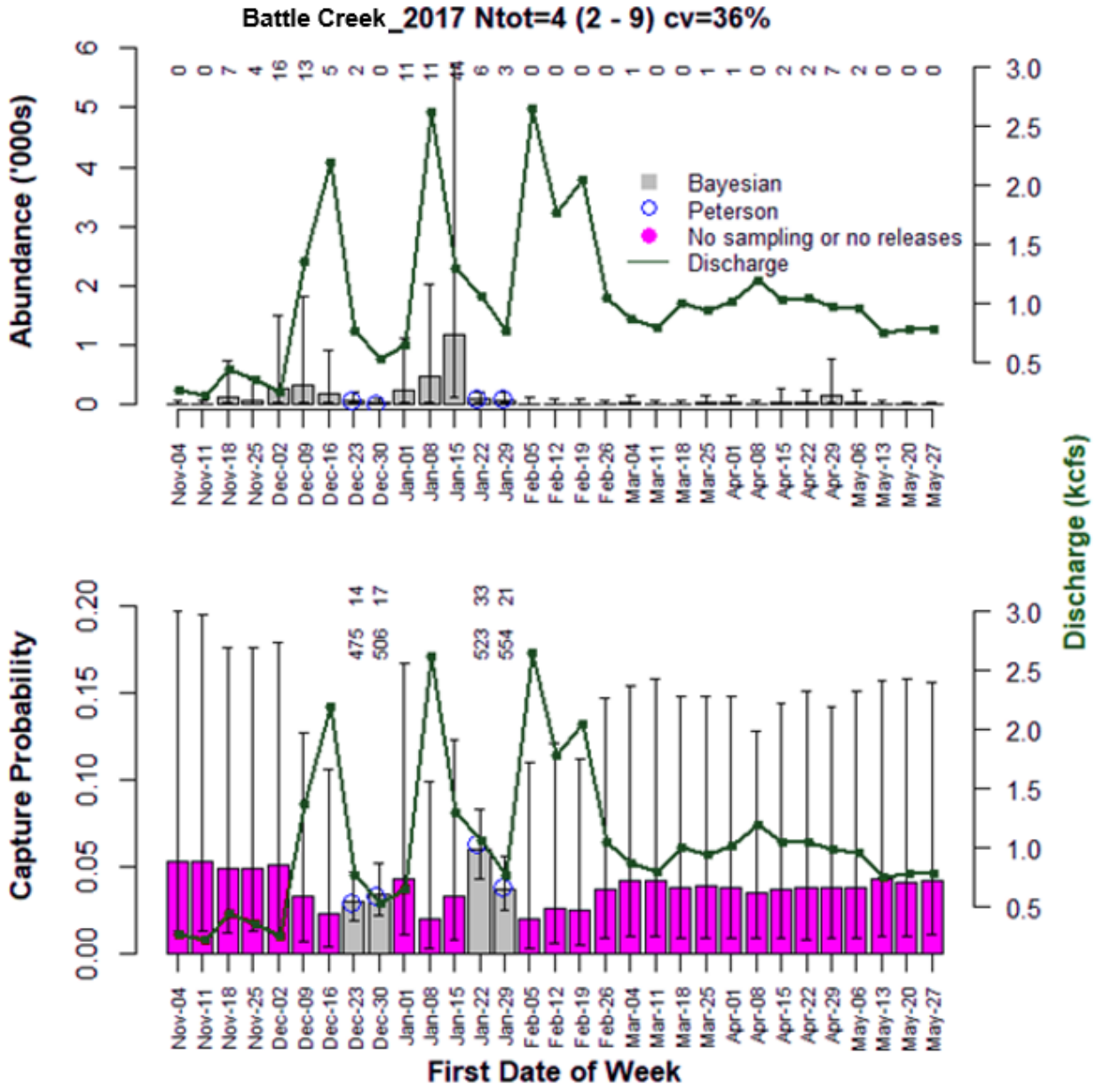

Figure 8, Continued

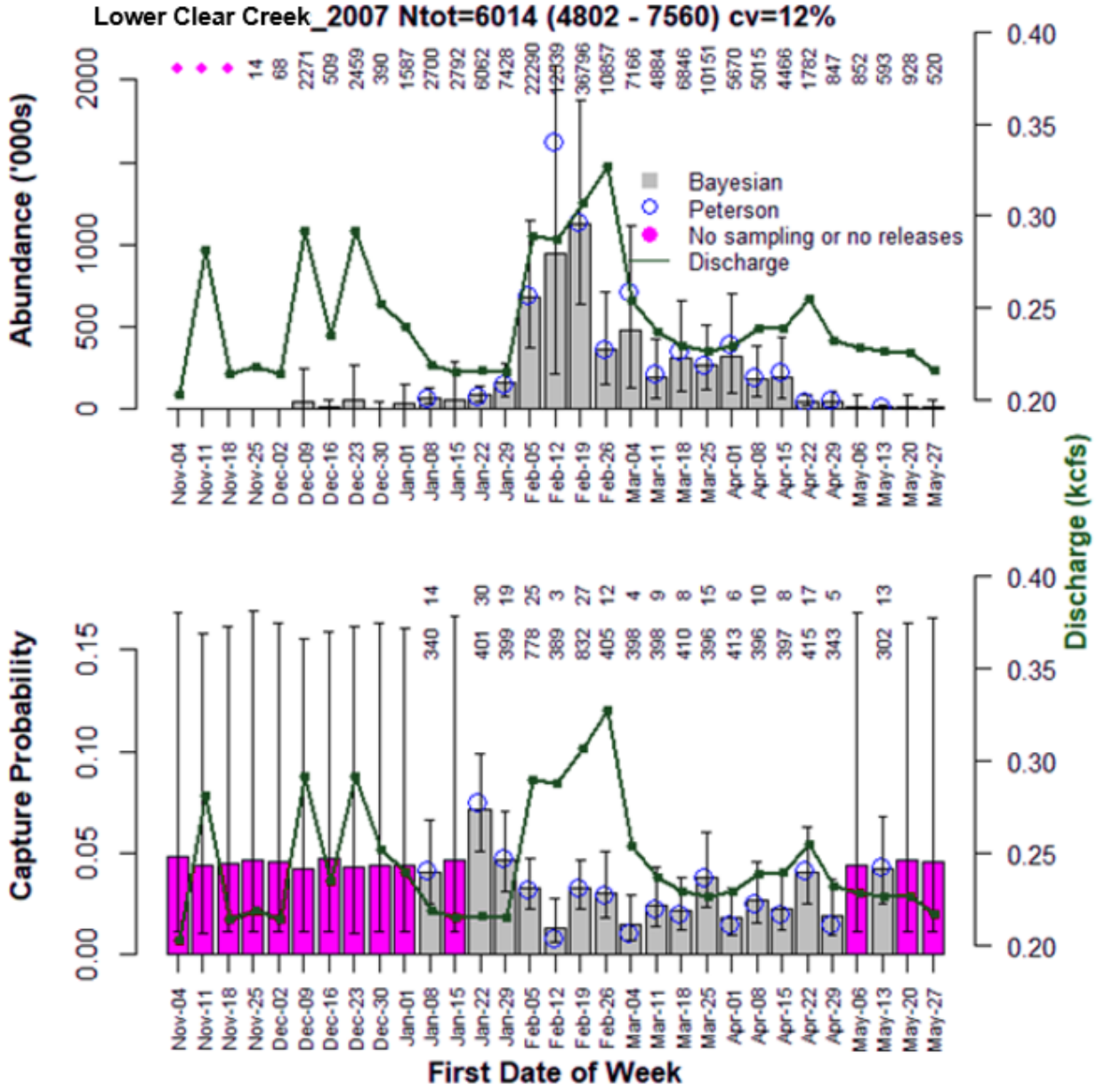

Figure 8, Continued

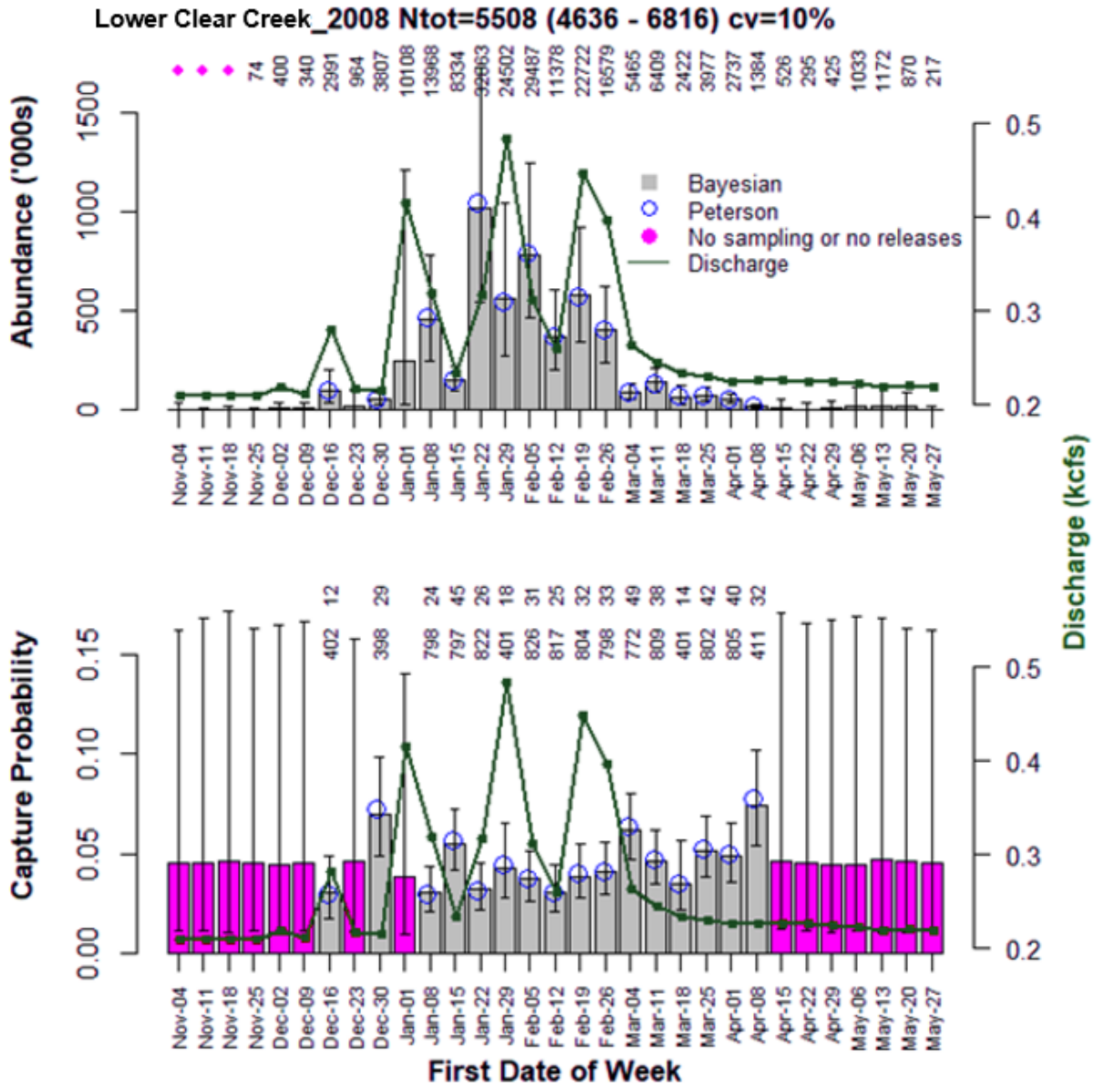

Figure 8, Continued

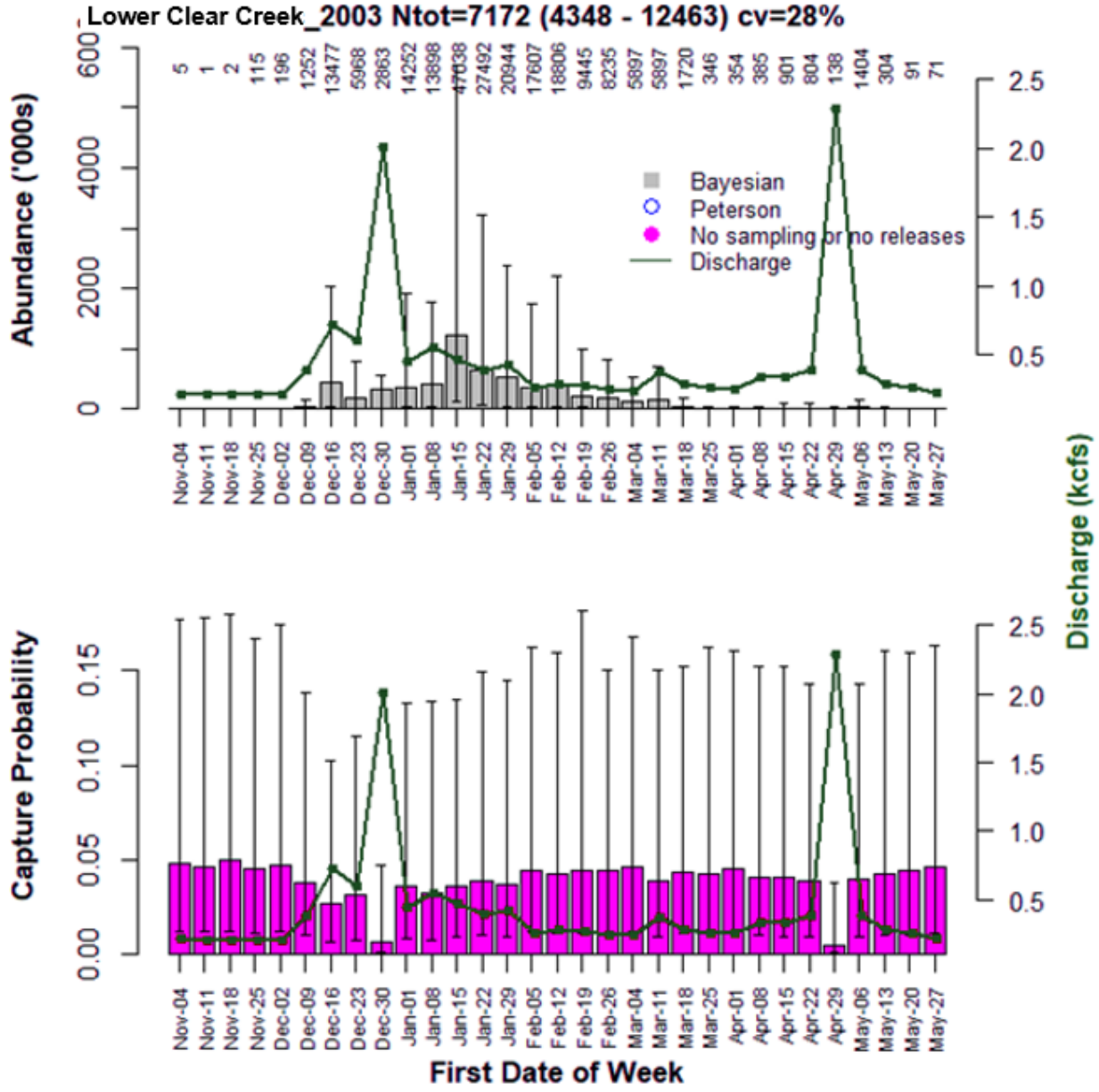

Figure 8, Continued

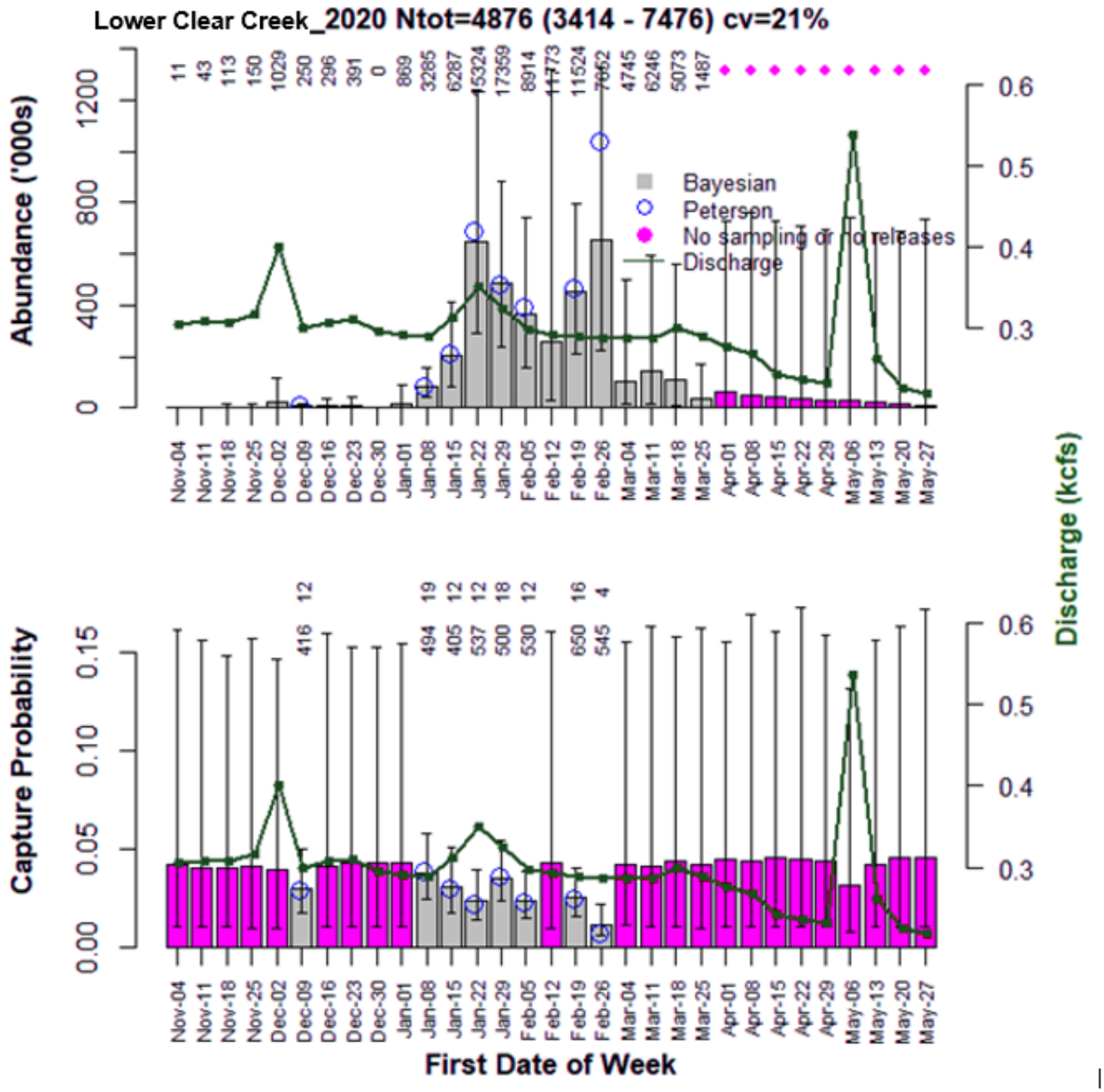

Figure 9. Time Series of Annual Juvenile Outmigrant Abundance Estimates Chinook Salmon (All Run Types)

Time series of annual (run year) juvenile outmigrant abundance estimates Chinook salmon (all run types) at six RST sites. The bar height and error bars represent the means and 95% credible intervals, respectively. The horizontal dashed line represents the mean across years.

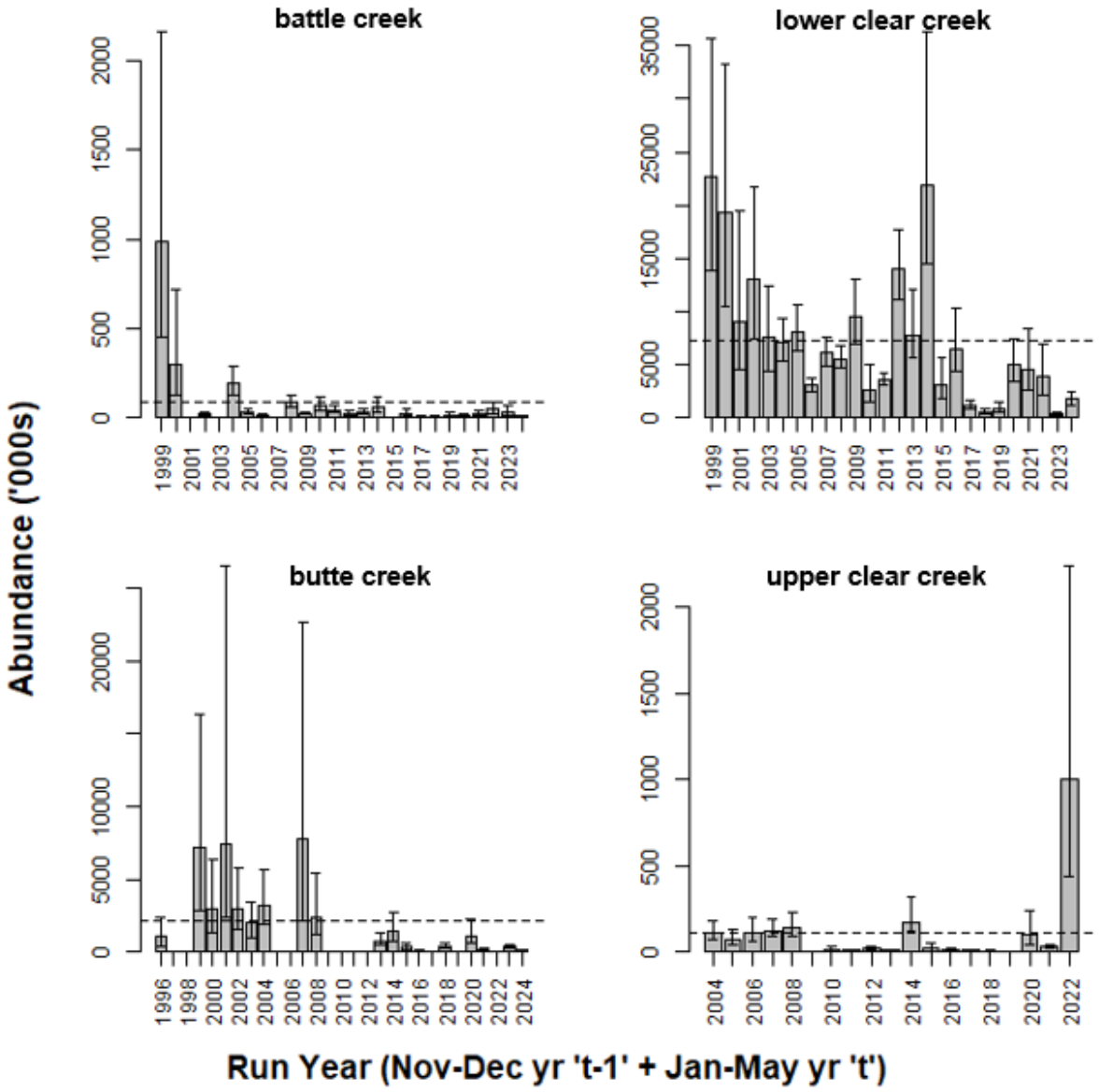

Figure 9, Continued

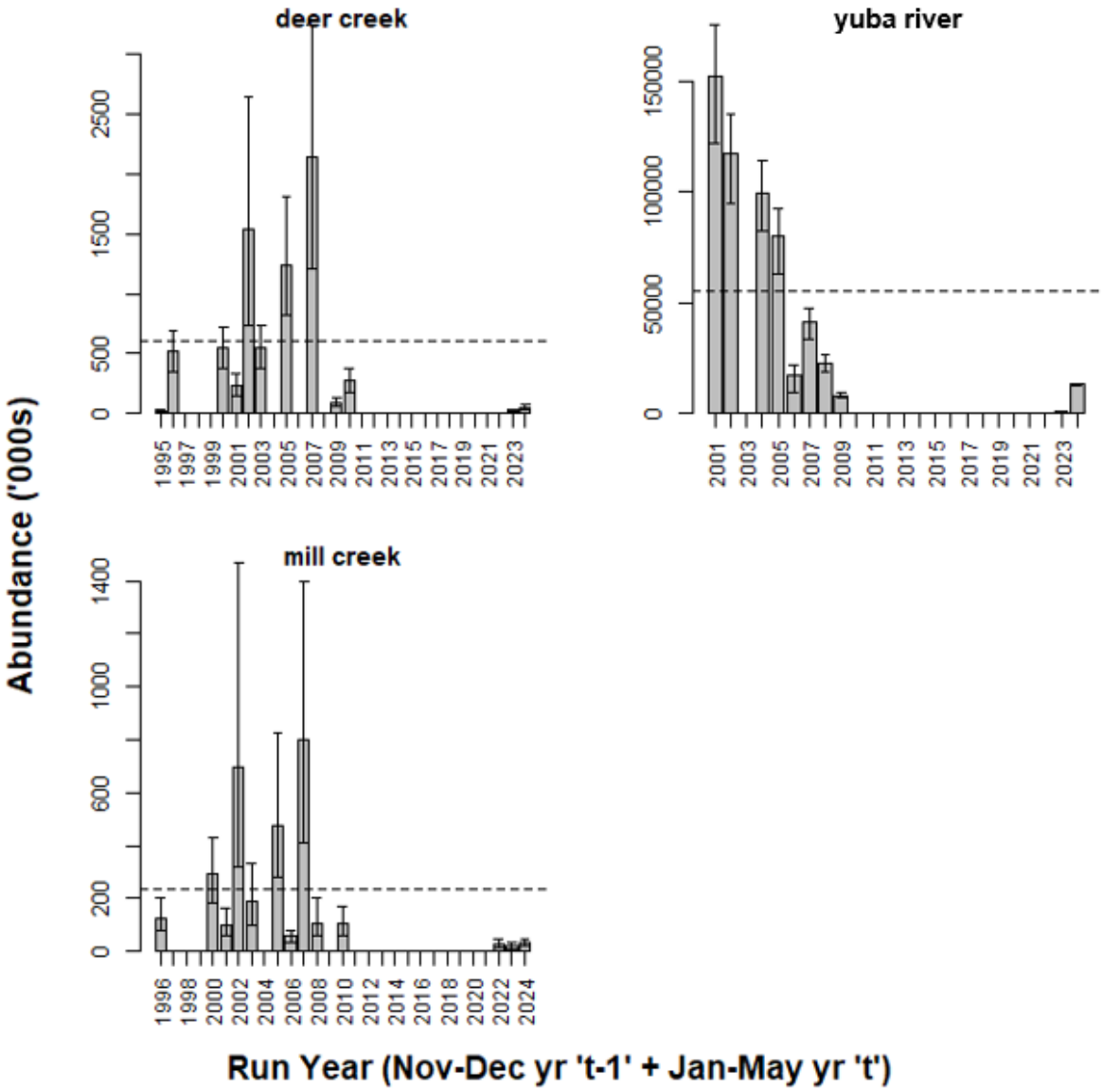

Figure 10. Weekly Abundance for Outmigrating Juvenile Chinook Salmon, Proportion of Spring-run from PLAD Model, and Resulting Abundance of Spring-run Outmigrants

Predicted weekly abundance for outmigrating juvenile Chinook salmon (all run types, top panel), the proportion of spring-run from the PLAD model (middle panel), and resulting abundance of spring-run outmigrant abundance (bottom panel) for Site LCC run year 2018. The bar height and error bars represent median values and 95% credible intervals, respectively. The titles for the top and bottom panels show the median, 95% credible interval (in parentheses), and the CV of the annual outmigrant abundance estimates.

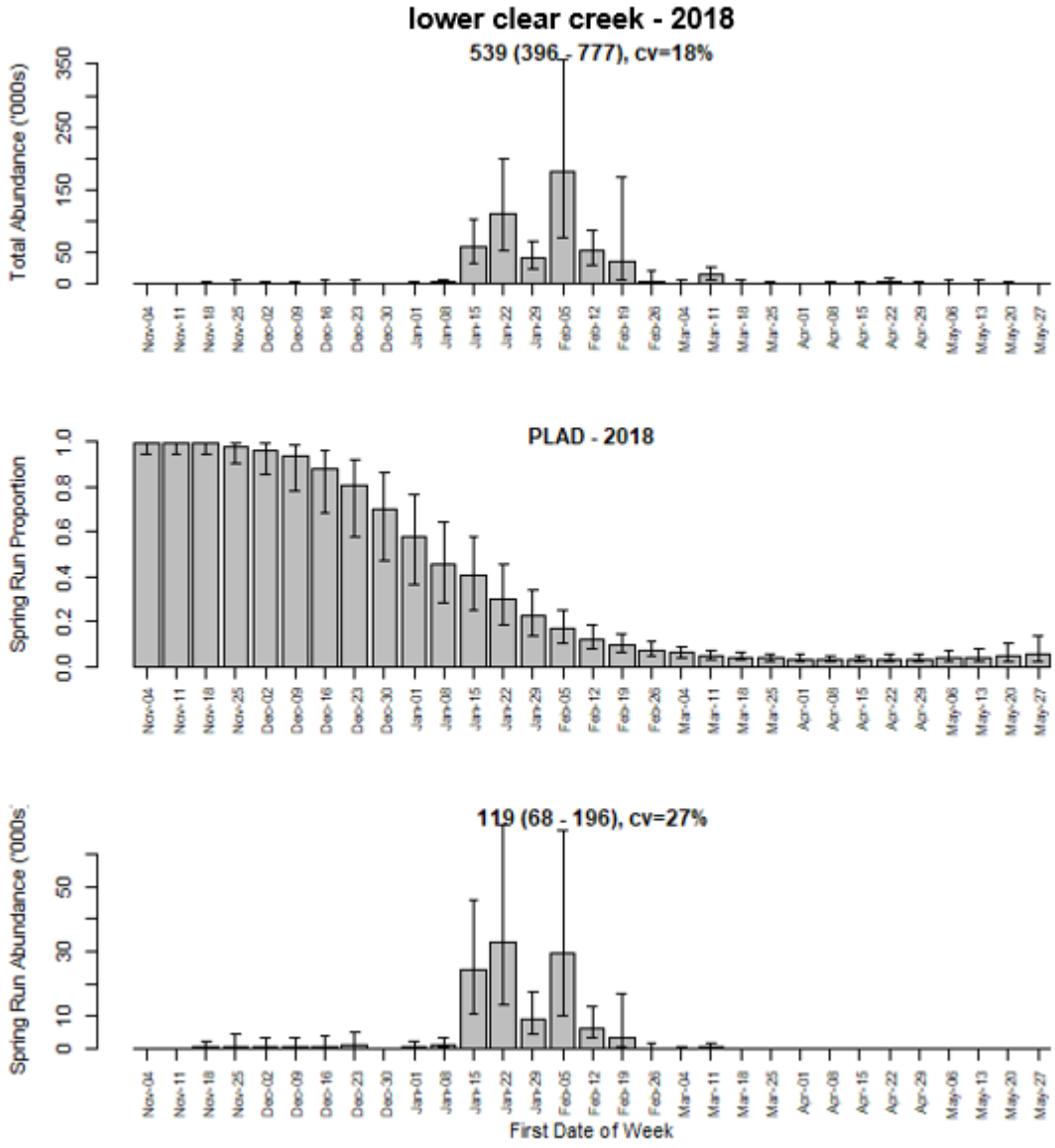

Figure 11. Time Series of Annual Juvenile Outmigrant Abundance Estimates for Spring-run Chinook Salmon

Time series of annual (run year) juvenile outmigrant abundance estimates for spring-run at six RST sites. The bar height and error bars represent the means and 95% credible intervals, respectively. The horizontal dashed line represents the mean across years.

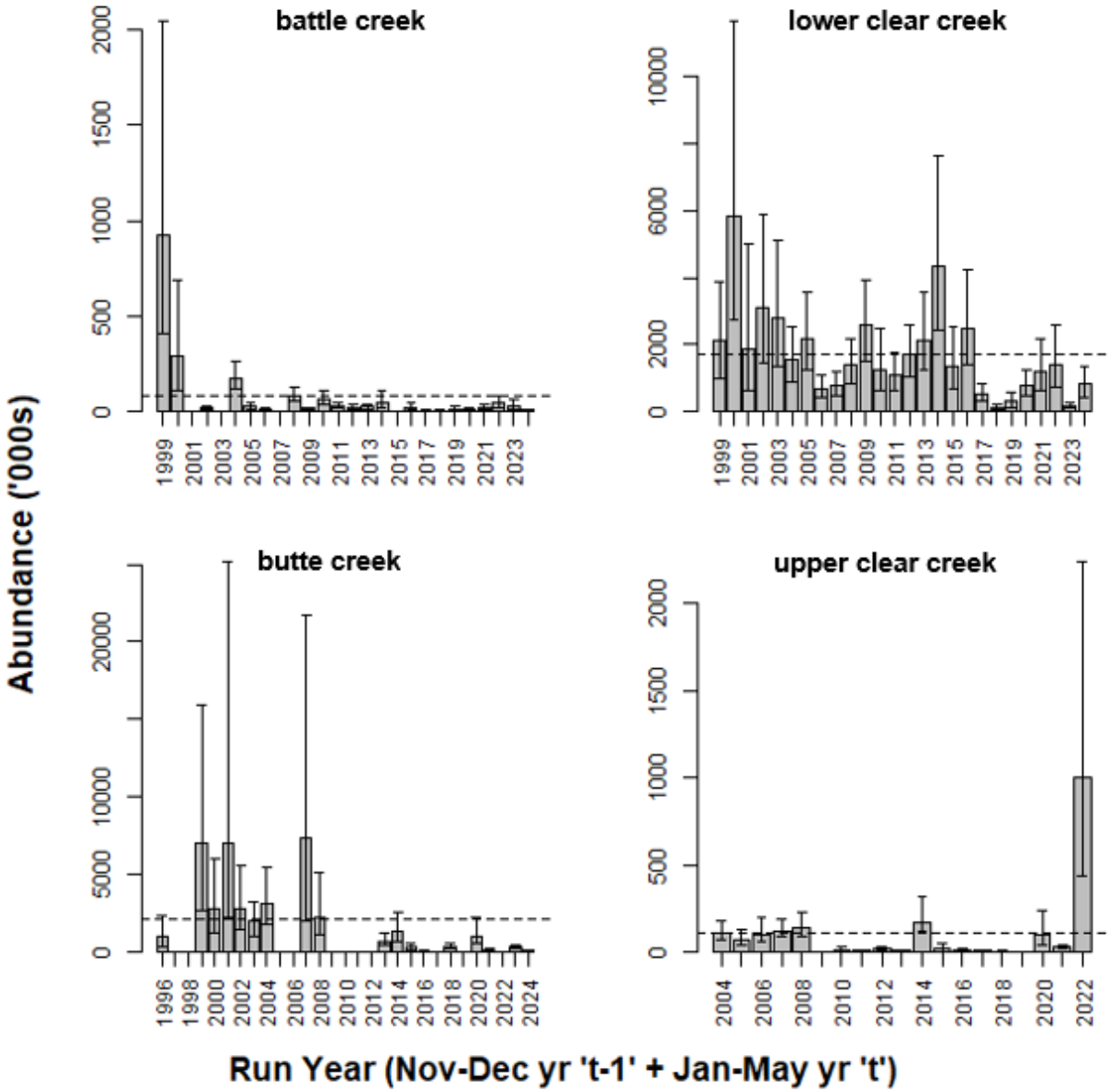

Figure 11. Continued

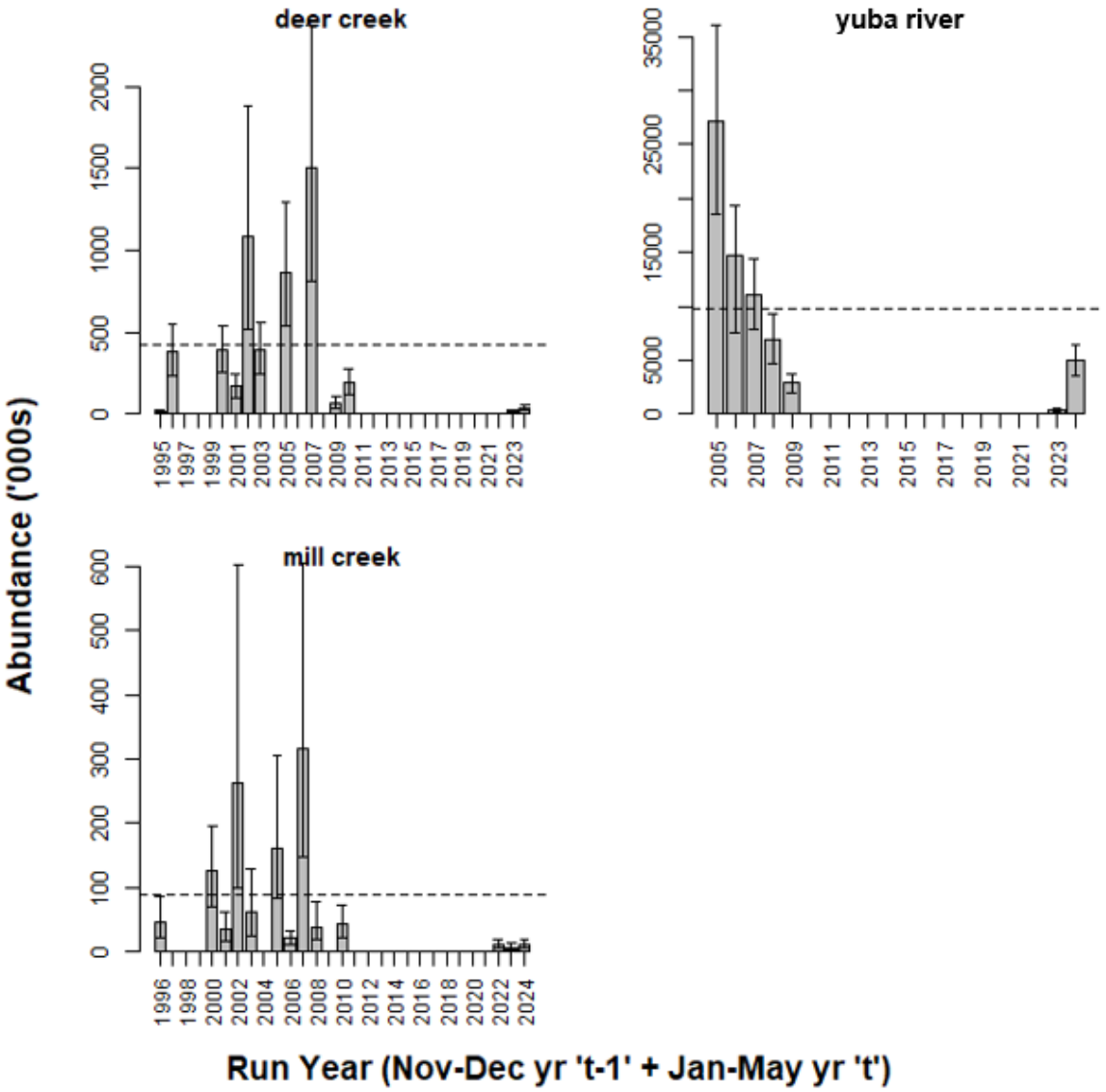

Figure 12. Comparison of Annual Spring-run Chinook Salmon Juvenile Outmigrant Estimates at the Upper Clear Creek and Lower Clear Creek Traps

Comparison of annual spring-run juvenile outmigrant estimates at Site UCC and LCC RSTs. Labels beside each point denote the run year. Dashed horizontal and vertical lines show the multi-year average abundance for Sites UCC and LCC, respectively.

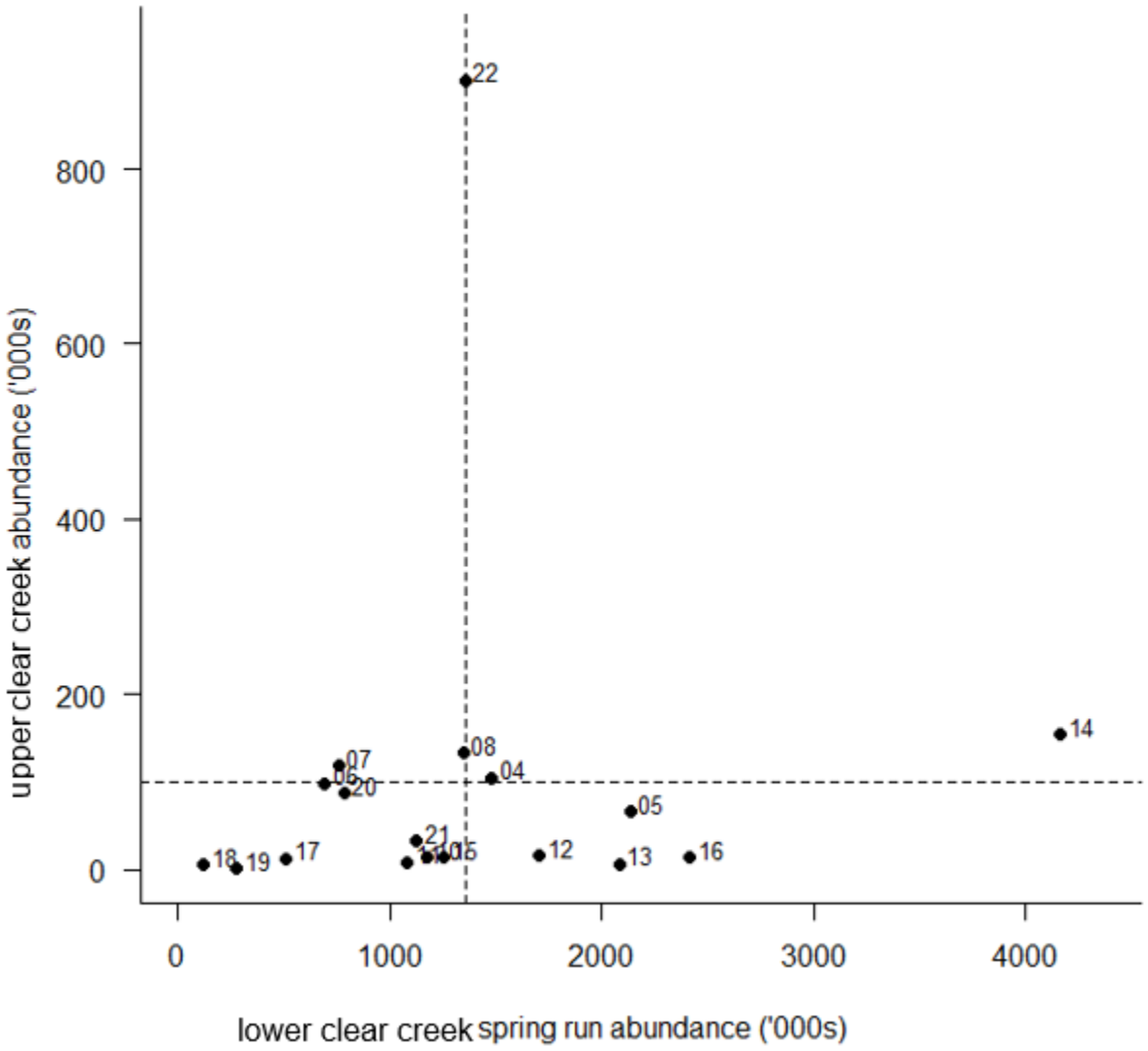

Appendices

A. Predictions of Weekly Capture Probabilities, Chinook Salmon Abundances (All Runs)

Plots of weekly abundance of juvenile Chinook salmon outmigrants (all run types combined) and capture probability for all site-years (trib_all.pdf)

B. Predictions of Weekly Probabilistic Length-at-Date Predictions and Spring-run Abundances

Plots of weekly abundance of juvenile Chinook salmon outmigrants (all run types combined), PLAD predictions of the proportion of spring-run salmon, and resulting predictions of spring-run outmigrant abundance (trib_sr.pdf)